appears to be widely observed in normal tissues, with particularly high levels detected in the placenta and lung.

SRPX2 expression was also examined in 30 human cancer cell lines, HUVEC and HEK293 cells. A relatively high *SRPX2* mRNA expression level was observed in gastric cancer (44As3, MKN7 and SNU-16), colorectal cancer (WiDr and COCM-1), lung cancer (PC-9), mesothelioma (MSTO), glioma (U251) and HUVEC. These results suggest that a variety of cancer and vascular endothelial cells express *SRPX2* (Fig. 1*b*).

TABLE I – *SRPX2* EXPRESSION AND PATIENT CHARACTERISTICS IN PATIENTS WITH GASTRIC CANCER

Characteristics	Patients No. (%)	*SRPX2* Expression (10^{-4}/*GAPD*)	*p* value
Age, years			
≥60	31 (54)	12.6 ± 12.5	0.10
<60	26 (46)	11.1 ± 9.1	
Sex			
Male	41 (72)	11.1 ± 9.1	0.61
Female	16 (28)	12.6 ± 12.5	
Histology[1]			
Diff.	22 (39)	11.3 ± 7.9	0.77
Undiff.	32 (56)	12.2 ± 11.7	
Prognosis[2]			
Favorable (≥6 months)	37 (65)	9.5 ± 7.2	<0.05
Unfavorable (<6 months)	20 (35)	15.1 ± 13.5	
Total	57		

[1]Histology of endoscopic samples divided into differentiated and undifferentiated type.–[2]Overall survival time from the first day of chemotherapy. A survival time of 6 months was used as the cut-off to divide patients into "Favorable" and "Unfavorable" groups.

Overexpression of SRPX2 mRNA in gastric cancer tissues

The expression of *SRPX2* mRNA was analyzed for paired tissues of gastric cancer and noncancerous gastric mucosa obtained from 24 gastric cancer patients. A paired *t* test demonstrated that *SRPX2* expression was significantly increased ($p = 0.0004$) in the cancerous tissues, compared to the noncancerous gastric mucosa (Fig. 1*c*). The *SRPX2* mRNA expression levels in the gastric cancer and noncancerous gastric mucosa were 6.6 ± 5.4 and 1.8 ± 1.2 ($\times 10^{-4}$/*GAPD*), respectively. Although the reason is unclear, 2 groups seemed to be present: 1 group with very high expression levels in cancerous tissues and another group with no difference in the expression levels between cancerous and noncancerous lesions.

To clarify the clinical significance of *SRPX2* expression, we examined the expression in an additional 57 gastric cancer samples using real-time RT-PCR and analyzed the correlations between *SRPX2* expression and clinical characteristics (Table I). Age, sex and histological cancer type were not correlated with *SRPX2* expression. However, patients with an unfavorable outcome, in whom the overall survival time (OS) was less than 6 months, exhibited significantly high expression levels of *SRPX2* in

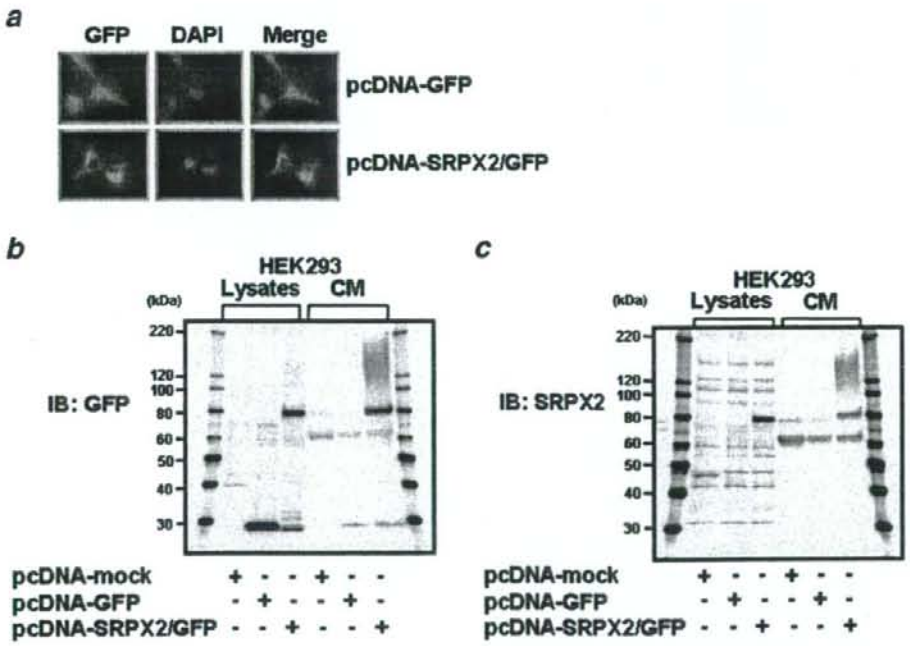

FIGURE 2 – Cellular distribution of SRPX2-GFP fusion protein. To examine the cellular distribution of SRPX2, we created cell lines expressing a fusion protein of SRPX2-GFP. The empty vector, GFP and SRPX2-GFP vectors were transfected into HEK293 cells using FuGENE6 transfection reagent. The vectors and stable transfectant cells in the HEK293 cells were designated as pcDNA-mock, pcDNA-GFP, pcDNA-SRPX2/GFP, HEK293-pcDNA-mock, HEK293-pcDNA-GFP and HEK293-pcDNA-SRPX2/GFP. (*a*) Fluorescence microscopy of HEK293-pcDNA-GFP (upper panel) and pcDNA-SRPX2/GFP cells (lower panel). The SRPX2/GFP fusion protein (green) showed a cytoplasmic distribution. The nucleus was stained by DAPI (blue). Western blot analysis detected by (*b*) anti-GFP antibody and (*c*) anti-SRPX2 antibody for HEK293-pcDNA-mock, HEK293-pcDNA-GFP and HEK293- pcDNA-SRPX2/GFP cells. Both the anti-GFP and the anti-SRPX2 antibodies detected the SRPX2-GFP fusion protein at ~80 kDa in the cell lysate and the secreted form at 150–180 kDa. IB, immunoblot; CM, culture medium.

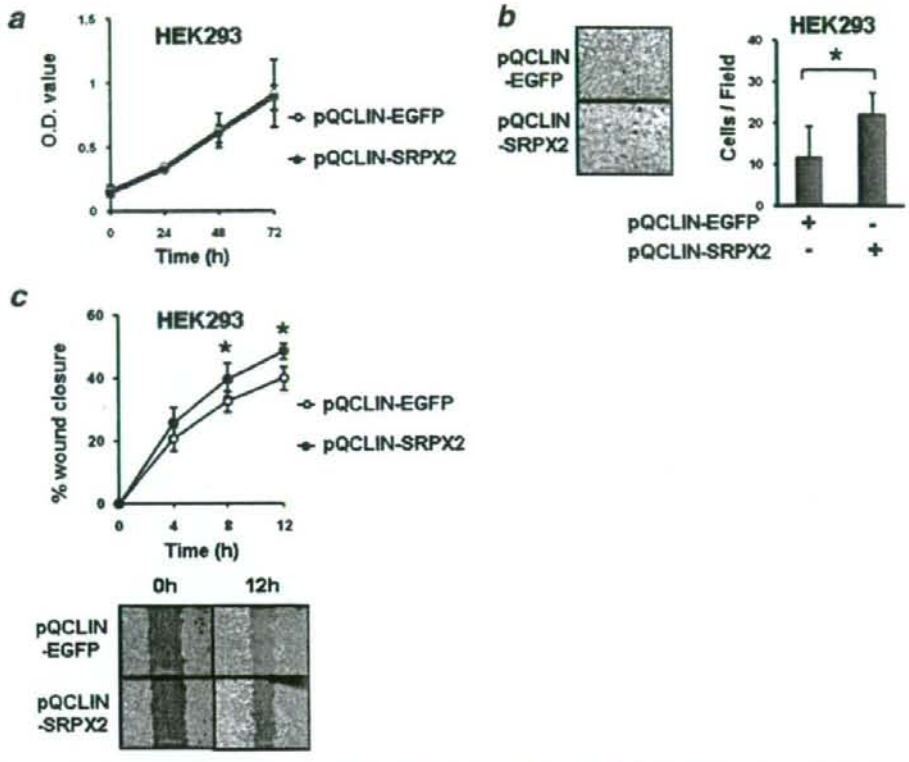

FIGURE 3 – SRPX2-introduced cells enhanced cellular migration but not cellular growth. Viral vectors containing EGFP and SRPX2 were constructed as pQCLIN-EGFP and pQLIN-SRPX2, respectively. These stable cell lines, retrovirally introduced into HEK293 cells, were designated as HEK293-pQCLIN-EGFP and HEK293-pQCLIN-SRPX2, respectively. (*a*) Cellular growth was examined using an MTT assay. No difference in cellular growth was observed between HEK293-pQCLIN-EGFP and HEK293-pQCLIN-SRPX2 cells. (*b*) Migration assay. Cells (2×10^4/well) were seeded into the upper chambers with serum-reduced medium (DMEM with 0.5% FBS). The upper chambers, with fibronectin coated on the outer side of the membrane, were then placed in the lower chambers of a 24-well culture plate containing DMEM with 10% FBS. After incubation for 8 hr at 37°C, medium was aspirated and the nonmigrated cells on the inner side of the membrane were removed using a cotton swab. The migrated cells on the outer side of the membrane were fixed, stained and counted using a light microscope. The experiment was performed in triplicate. The left panels show representative data. (*c*) Wound healing assay for HEK293-pQCLIN-EGFP and HEK293-pQCLIN-SRPX2 cells. Wounds were introduced to the confluent cell monolayer using a plastic pipette tip. After 4, 8 and 12 hr, the wound area was photographed and measured. The lower panels show representative data. The experiment was performed in triplicate. *: $p < 0.05$. EGFP, enhanced green fluorescent protein.

cancerous tissues ($p < 0.05$). The *SRPX2* expression levels in patients with an unfavorable outcome (OS < 6 months) and in those with a favorable outcome (OS > 6 months) were 9.5 ± 7.2 and 15.1 ± 13.5 ($\times 10^{-4}$/*GAPD*), respectively. This result suggests that *SRPX2* might be a prognostic biomarker, that is, associated with a malignant phenotype in gastric cancer.

SRPX2 is secreted into culture medium and localized in cytoplasm

Because the cellular distribution of an uncharacterized protein often suggest its biological function (*e.g.*, transcription factors tend to be localized in the nucleus), we tried to identify the cellular distribution of SRPX2 using a SRPX2-GFP fusion protein. We introduced an empty vector, GFP, or SRPX2 fused with GFP into HEK293 cells to create the following stable cell lines: HEK293-pcDNA-mock, HEK293-pcDNA-GFP and HEK293- pcDNA-SRPX2/GFP, respectively. The SRPX2-GFP fusion protein exhibited a cytoplasmic distribution (Fig. 2*a*). The protein expression of SRPX2 was then analyzed using western blotting and both anti-GFP and anti-SRPX2 antibodies (Figs. 2*b* and 2*c*). Western blotting with anti-GFP antibody revealed that an SRPX2-GFP fusion protein with a molecular weight (M.W.) of ~80 kDa was detected in both the cell lysates and the culture medium. A similar result was observed using anti-SRPX2 antibody. In addition, an SRPX2/GFP protein with a molecular weight of 150–180 kDa was observed in the culture medium when analyzed using both anti-GFP and anti-SRPX2 antibodies. The SRPX2 protein was detected as 2 bands with molecular weights of ~80 kDa and 150–180 kDa (containing a GFP protein of 30 kDa). The band was consistent with the estimated molecular weight of SRPX2, 53 kDa. The higher band was only observed in the culture medium and was detected using both anti-GFP and anti-SRPX2 antibodies.

SRPX2-introduced cells enhanced cellular migration but not cellular growth

To elucidate the biological function of SRPX2, EGFP or SRPX2 was retrovirally introduced into HEK293 cells. The stable cell lines were designated as HEK293-pQCLIN-EGFP and HEK293-pQCLIN-SRPX2, respectively. We then performed cellular growth assays using these cells (Fig. 3*a*). No difference in

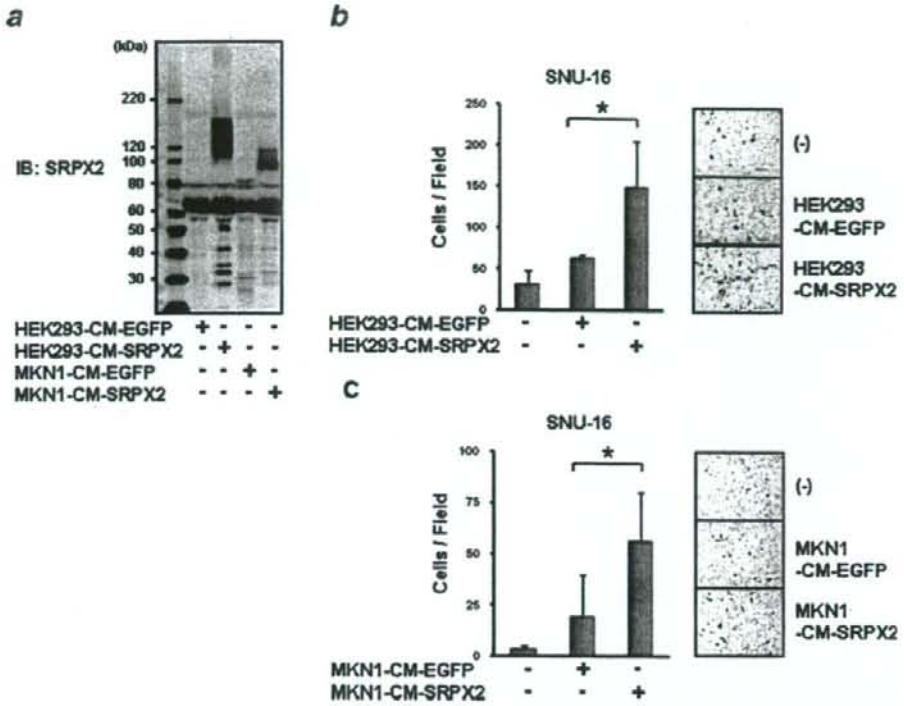

FIGURE 4 – SRPX2-conditioned medium enhanced cellular migration. (*a*) Western blotting for conditioned medium obtained from the stable cell lines, HEK293-pQCLIN-EGFP, HEK293-pQCLIN-SRPX2, MKN1-pQCLIN-EGFP and MKN1-pQCLIN-SRPX2. Each concentration of conditioned medium was adjusted to 1 mg/mL and diluted before use. Further details are described in the "Material and methods" section. IB, immunoblotting; HEK293-CM-EGFP, conditioned medium from HEK293-pQCLIN-EGFP cells; HEK293-CM-SRPX2, conditioned medium from HEK293-pQCLIN-SRPX2 cells; MKN1-CM-EGFP, conditioned medium from MKN1-pQCLIN-EGFP cells; MKN1-CM-SRPX2, conditioned medium from MKN1-pQCLIN-SRPX2 cells. The role of SRPX2 in cellular migration was assessed in the gastric cancer cell line, SNU-16, using a migration assay and EGFP- or SRPX2-conditioned medium from (*b*) HEK293-pQCLIN-EGFP or -SRPX2 cells and from (*c*) MKN1-pQCLIN-EGFP or -SRPX2 cells. A total of 1×10^5 SNU-16 cells were seeded into the upper chambers with 200 μL of RPMI containing 0.5% FBS. The final concentration of 100 μg/mL of EGFP-conditioned or SRPX2-conditioned medium was added to the 600 μL volume of the RPMI1640 containing 0.5% FBS medium in the lower chamber of the 24-well culture dish. The cells were incubated for 24 hr at 37°C. The number of migrated cells was evaluated as described earlier. The experiment was performed in triplicate. Representative data is shown in the right panels. The SRPX2-conditioned medium significantly enhanced cellular motility ($p < 0.05$) by about 2-fold, compared to the EGFP-conditioned medium. Data are shown as the mean ± SD of 3 independent experiments. *: $p < 0.05$.

cellular growth was seen between the cells, indicating that SRPX2 is not involved in cellular growth in HEK293 cells.

We next performed a migration assay to assess the role of SRPX2 in cellular motility. The cellular migration activity of the HEK293-pQCLIN-SRPX2 cells was significantly enhanced, compared to the EGFP transfectant cells ($p = 0.03$, Fig. 3*b*). A wound healing assay also demonstrated that the cellular motility of HEK293-pQCLIN-SRPX2 cells was significantly enhanced, compared to that of EGFP transfectant cells, at 8 and 12 hr after wound infliction ($p < 0.05$, Fig. 3*c*). Although the actual difference in the wound healing assay result was relatively small, these results indicate that SRPX2 is involved in cellular motility.

SRPX2-conditioned medium enhanced cellular migration

EGFP or SRPX2 was also introduced into a gastric cancer cell line, MKN1, and the SRPX2-conditioned media obtained from MKN1 and HEK293 cells were subjected to a migration assay. The transfected cells mainly produced the secreted type of SRPX2 protein with the higher molecular weight, as detected using western blot analysis. The SRPX2 proteins produced by MKN1 and HEK293 cells were observed at ~95 kDa and 110–150 kDa, respectively (Fig. 4*a*). This difference in molecular weight might be due to glycosylation.

The role of the secreted SRPX2 protein in the conditioned medium on cellular migration was assessed to SNU-16 cells using a migration assay. SNU-16 cells were incubated for 24 hr in a normal culture medium containing 100 μg/mL of EGFP- or SRPX2-conditioned medium from HEK293-pQCLIN-EGFP or -SRPX2 cells added to the lower chamber of the 24-well culture dish. The SRPX2-conditioned medium significantly enhanced the cellular motility of the SNU-16 cells ($p < 0.05$) by about 2-fold higher than that of the EGFP-conditioned medium (Fig. 4*b*). Similar results were observed using conditioned medium from MKN1-pQCLIN-EGFP or -SRPX2 cells (Fig. 4*c*). This result indicates that the secreted SRPX2 protein increased cellular motility in gastric cancer cells.

SRPX2 protein promoted cellular attachment

We examined the cellular adhesion potential of 7 gastric cancer cell lines cultured on EGFP- and SRPX2-conditioned medium-

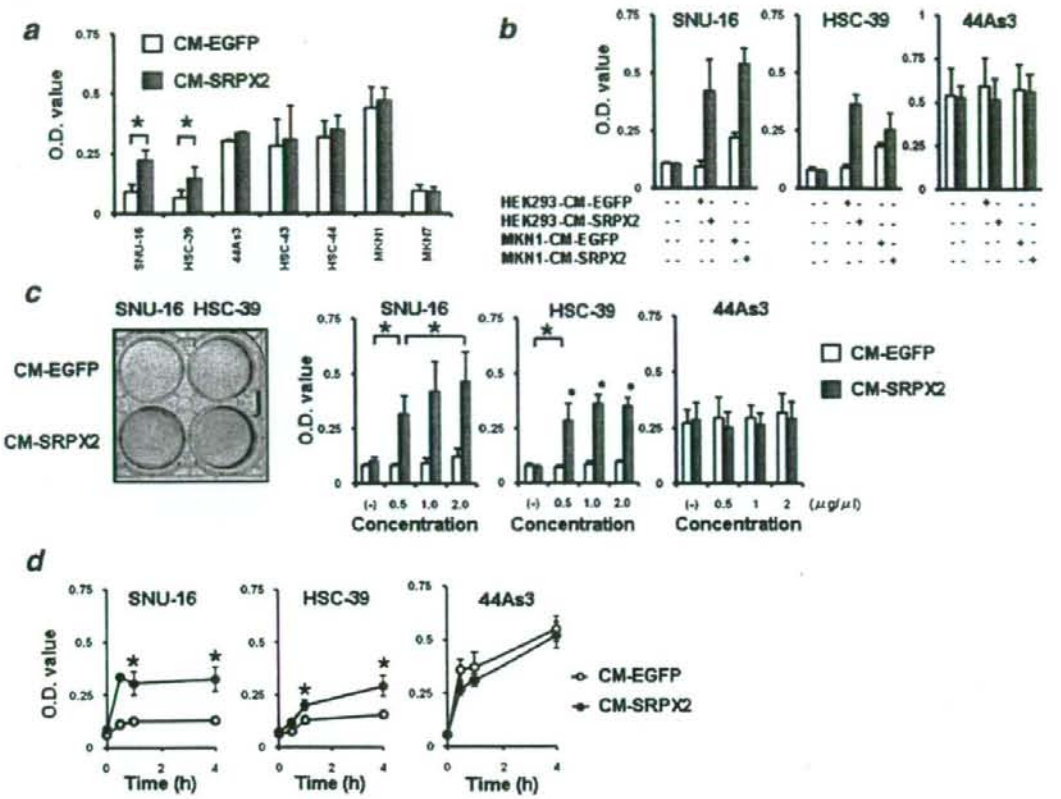

FIGURE 5 – SRPX2 protein enhanced cellular attachment. EGFP-conditioned or SRPX2-conditioned medium was adjusted to a concentration of 1 mg/mL and 50 μL was placed at 4°C overnight on 96-well plates. The conditioned medium was aspirated, and the wells were washed twice with phosphate-buffered saline (PBS). The plates were used in the adhesion assay as conditioned medium-coated 96-well plates. The cells to be analyzed (2×10^4 cells /well) were seeded into the wells of conditioned medium-coated plates and incubated at 37°C for 1 hr. The wells were then washed twice with PBS to remove nonadherent cells. The adherent cells were evaluated using an MTT assay. (*a*) A cellular adhesion assay was performed using 7 gastric cancer cell lines and conditioned medium-coated plates. The numbers of adhered SNU-16 and HSC-39 cells were significantly larger with the SRPX2-conditioned medium coated-plates ($p < 0.05$). (*b*) A cellular adhesion assay was also performed using conditioned medium-coated plates obtained from MKN1-pQCLIN-EGFP and MKN1-pQCLIN-SRPX2 cells. The numbers of adhered SNU-16 and HSC-39 cells, but not 44As3 cells, were significantly larger. (*c*) A cellular adhesion assay was performed using different concentrations of conditioned medium-coated plates. The 6-well-plate-scale data is shown in the left panel. (*d*) Cellular adhesion assay for time-course analysis. Larger numbers of attached SNU-16 and HSC-39 cells were observed from 0.5 to 4 hr. The increase in cellular attachment induced by the SRPX2 protein emerged after a relatively short time (0.5 hr). The experiment was performed in triplicate. CM-EGFP, conditioned medium from HEK293-pQCLIN-EGFP cells; CM-SRPX2, conditioned medium from HEK293-pQCLIN-SRPX2 cells. [Color figure can be viewed in the online issue, which is available at www.interscience.wiley.com.]

coated plates. Five of the gastric cancer cell lines did not increase cellular attachment to the conditioned medium-coated plate. However, the numbers of attached SNU-16 and HSC-39 cells were significantly increased by more than 2-fold by the presence of SRPX2 protein ($p < 0.05$, Fig. 5*a*).

To exclude nonspecific effects, cellular adhesion assays were also performed using conditioned medium-coated plates obtained from MKN1-pQCLIN-EGFP and MKN1-pQCLIN-SRPX2 cells (Fig. 5*b*). The SNU-16 and HSC-39 cells, but not the 44As3 cells, also exhibited a significantly larger number of adhered cells in the presence of SRPX2 protein obtained from the conditioned-medium of MKN1 cells. Cellular adhesion in these 3 cell lines was examined using 4 different concentrations of conditioned medium-coated plates. Similar results were obtained, and a dose-response effect for the conditioned medium was observed in SNU-16 cells (Fig. 5*c*). Time-course experiments revealed that a larger number of attached SNU-16 and HSC-39 cells were observed after a short time (0.5 hr) to 4 hr after the start of incubation (Fig. 5*d*). Microscopic examination revealed that most of the adhered cells did not exhibit "cell spreading" and instead resembled "cellular attachment." These results demonstrate that SRPX2 is involved in cellular attachment in SNU-16 and HSC-39 cells.

SRPX2 protein increased phosphorylation levels of FAK

FAK plays a key role in cellular adhesion, and FAK signaling is considered to be a major pathway.[11] To gain insight into the function of SRPX2, the phosphorylation levels of FAK in SNU-16 cells were examined after culturing in a medium to which SRPX2-conditioned medium had been added. Increased phosphorylation levels of FAK (pY397 and pY576/577) were observed in SNU-16 cells in the presence of SRPX2, compared to EGFP, after 1–12 hr of culture (Fig. 6*a*). FAK phosphorylation occurred during an early stage (1 hr) and was consistent with the results for cellular

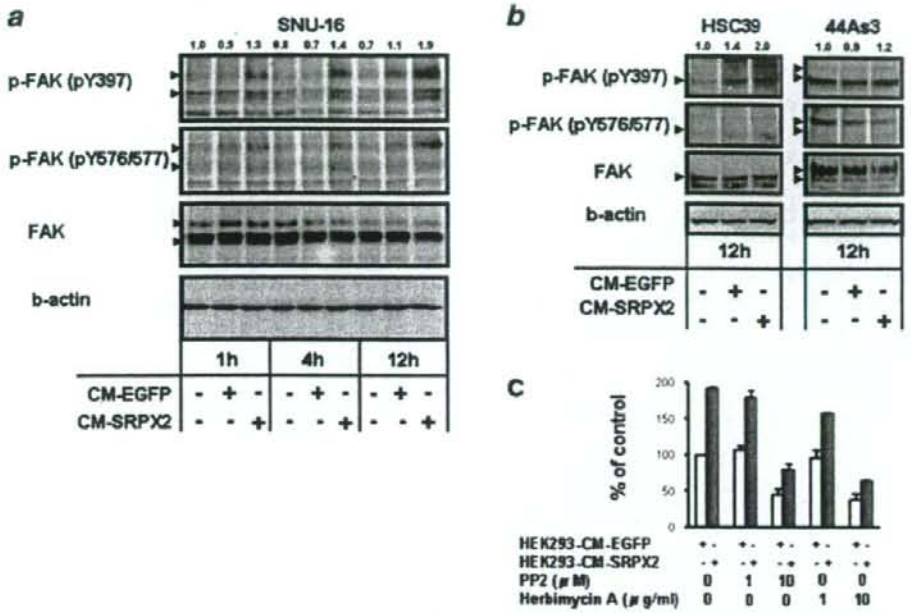

FIGURE 6 – SRPX2 protein increased the phosphorylation levels of FAK. The SNU-16 cells were cultured in RPMI with 0.5% FBS under the presence of GFP or SRPX2-conditioned medium at a final concentration of 100 μg /mL. The cells were collected at 1, 4 and 12 hr after incubation. Ten micrograms of cell lysate were subjected to western blotting using anti-phospho-FAK (pY397 and pY576/577), anti-FAK and anti-β-actin antibodies. A western blot was performed for (*a*) SNU-16 cells, and (*b*) HSC-39 and 44As3 cells. FAK, focal adhesion kinase; CM-EGFP, conditioned medium from HEK293-pQCLIN-EGFP cells; CM-SRPX2, conditioned medium from HEK293-pQCLIN-SRPX2 cells. Arrowheads: target molecules. The numerical densitometrical data of phospho-FAK (pY397) is shown above the western blot. (*c*) SNU-16 cells were treated with FAK inhibitors (PP2; final concentrations 1 or 10 μM and Herbimycin A; final concentrations 1 or 10 μg/mL) in a cellular adhesion assay to assess SRPX2-mediated attachment. Both PP2 and Herbimycin A inhibited cellular attachment of SNU-16 cells in dose-dependent manners. [Color figure can be viewed in the online issue, which is available at www.interscience.wiley.com.]

attachment. FAK phosphorylation by SRPX2 was also stimulated in HSC-39 cells but not in 44As3 cells (Fig. 6*b*). In addition, to determine whether FAK inhibitors could affect the SPRX2-mediated cellular attachment, the SNU-16 cells were treated with PP2[12] and Herbimycin A[13] to inhibit FAK activity in cellular adhesion assay (Fig. 6*c*). PP2 and Herbimycin A inhibited cellular attachment of SNU-16 cells in dose-dependent manners.

Although the molecules that transduce the extracellular SRPX2 signal into an intracellular signal remain unknown, these results suggest that the cellular phenotype caused by SRPX2 is associated with the FAK signaling pathway.

Discussion

Considering the structural features of *SRPX2*, the presence of both the sushi-repeat domain and the HYR domains predict an adhesive function.[4,8] We demonstrated that *SRPX2* enhanced cellular motility and cellular attachment, and these findings were consistent with the structural prediction.

The selectin family is the closest family to *SRPX2* and *SRPX*.[3] Selectins are known as cellular adhesion molecules and play key roles in the mediation of early neutrophil rolling on and adherence to endothelial cells.[14] Selectins recognize glycosylated proteins or lipids as their ligands, and this modification is necessary for their interaction.[15] The phylogenetical similarity between *SRPX2* and selectins suggests a similar biological function. SNU-16 and HSC-39 cells are basically nonadherent, and the increase in their cellular attachment was a relatively rapid response (0.5 hr). While number of attached cells increased significantly, the attachments were weak and the cells did not spread on the plates. Thus, the increased cellular attachment induced by SRPX2 seems to resemble neutrophil rolling.

Because the DGEA motif is a potential integrin-binding motif[16] and this motif exists in the first sushi domain of SRPX2, we hypothesized that this motif is a critical binding site for SRPX2's ability to enhance cellular migration and attachment. We examined the inhibitory effect of the DGEA peptide[16] on cell migration and attachment, but no inhibitory effect was observed (data not shown). This result suggests that the cell migration and attachment induced by SRPX2 might be independent of DGEA sequence-mediated signal transduction, or such a sequon does not function in SRPX2.

FAK is a major focal adhesion-associated protein that transmits signals downstream of integrins. FAK signals control important biological events, including cell migration, proliferation and survival, through downstream molecules like Rho, Rac, Rap1, CDC42 and PAK.[11,17,18] Our results demonstrated that SRPX2 protein increased the phosphorylation levels of FAK in SNU-16 and HSC-39 cells, but not in 44As3 cells (Figs. 6*a* and 6*b*), and enhanced the cellular adhesive potential in SNU-16 and HSC-39 cells but not in 5 other cell lines (Fig. 5*a*). We speculate that certain molecules overexpressed in SNU-16 and HSC-39 cells may localize on the cell surface and bind to SRPX2 protein, activating FAK signaling. Recently, Royer-Zemmour *et al.*[19] demonstrated the interaction of SRPX2 with uPAR (plasminogen activator, urokinase receptor) as well as with other partners such as cathepsin B. Because uPAR particularly plays an important and well-known role in various tumoral processes including cell proliferation, migration, invasion and adhesion, and because uPAR-associated

intracellular signaling may act through FAK. The SRPX2/uPAR interaction might provide a possible molecular explanation for the role of SRPX2 in cancer.

Regarding the higher fuzzy smeared-band observed in only the culture medium (Figs. 2*b*, 2*c* and 4*a*), the size of the bands differed considerably between HEK293 and MKN1 cells (110–150 kDa and ~95 kDa, respectively). These results suggest that the higher smeared bands are probably not dimmers, but they may represent a highly glycosylated protein modification. We tried to cut off the N-glycans using N-glycosidase F, but the 150-kDa smeared band did not disappear. We plan to perform additional experiments to clarify the cause of the smeared band in future studies, the results of which will undoubtedly be useful in predicting the function of SRPX2.

Many studies have indicated that selectins, the family most similar to SRPX and SRPX2 proteins, increase the interaction between tumor cells and endothelial cells, leading to tumor progression and metastasis.[20,21] Thus selectins are considered promalignancy factors.[20] Recent reports have shown that selectins positively promote angiogenesis.[22,23] Because HUVEC cells express high levels of *SRPX2* mRNA, the involvement of *SRPX2* in angiogenesis should be clarified.

In this study, we demonstrated that *SRPX2* is overexpressed in gastric cancer, compared to noncancerous gastric mucosa from the same patients, at the transcriptional level. A real-time RT-PCR analysis of 32 cell lines revealed that other cancer cells also express high levels of *SRPX2* mRNA. *SRPX2* was also overexpressed by more than 10-fold in clinical samples of colorectal cancers, compared to paired colonic mucosa (unpublished data). Thus, *SRPX2* overexpression in cancer tissue may not be restricted to gastric cancers. We plan to further examine *SRPX2* expression using immunohistochemistry in clinical samples of other cancers in the future.

Although the meaning of *SRPX2* overexpression in gastric cancer is unclear, a real-time RT-PCR analysis of clinical samples showed that *SRPX2* expression is associated with a poor prognosis in patients with gastric cancer. *SRPX2* was first identified as a downstream molecule of *E2F-HLF* in pro-B acute leukemia with t(17;19) (q23;p13) and has since been reported to contribute to malignant phenotypes.[1] *E2F-HLF*-positive leukemia is characterized by a poor outcome with bone invasion, hypercalcemia and intravascular coagulation.[24] The clinical features of leukemia and our results for gastric cancer suggest that the biological function of *SRPX2* is concerned with oncogenic activity. Further investigations of clinical outcome in relation to *SRPX2* expression are needed.

In conclusion, we found that *SRPX2* is overexpressed in gastric cancer and plays roles in cellular migration and adhesion in cancer cells. These results provide novel insight into the biological function of *SRPX2* in cancer cells.

Acknowledgements

This work was supported by funds for the Third-Term Comprehensive 10-Year Strategy for Cancer Control and the program for the promotion of Fundamental Studies in Health Sciences of the National Institute of Biomedical Innovation (NoBio) and the Japan Health Sciences Foundation. The following people have played very important roles in the conduct of this project. Miss Hiromi Orita, Dr. Hisanao Hamanaka, Dr. Ayumu Goto, Dr. Hisateru Yasui, Dr. Junichi Matsubara, Dr. Natsuko Okita, Dr. Takako Nakajima, Dr. Atsuo Takashima, Dr. Kei Muro, Dr. Takashi Ura, Miss Hideko Morita, Miss Mari Araake, Dr. Hisao Fukumoto, Dr. Tatsu Shimoyama, Dr. Naoki Hayama, Dr. Masayuki Takeda, Dr. Hideharu Kimura, Miss Kazuko Sakai, Dr. Terufumi Kato and Dr. Jun-ya Fukai.

References

1. Kurosawa H, Goi K, Inukai T, Inaba T, Chang KS, Shinjyo T, Rakestraw KM, Naeve CW, Look AT. Two candidate downstream target genes for E2A-HLF. Blood 1999;93:321–32.
2. Roll P, Rudolf G, Pereira S, Royer B, Scheffer IE, Massacrier A, Valenti MP, Roeckel-Trevisiol N, Jamali S, Beclin C, Seegmuller C, Metz-Lutz MN, et al. SRPX2 mutations in disorders of language cortex and cognition. Hum Mol Genet 2006;15:1195–207.
3. Royer B, Soares DC, Barlow PN, Bontrop RE, Roll P, Robaglia-Schlupp A, Blancher A, Levasseur A, Cau P, Pontarotti P, Szepetowski P. Molecular evolution of the human SRPX2 gene that causes brain disorders of the Rolandic and Sylvian speech areas. BMC Genet 2007;8:72.
4. O'Leary JM, Bromek K, Black GM, Uhrinova S, Schmitz C, Wang X, Krych M, Atkinson JP, Uhrin D, Barlow PN. Backbone dynamics of complement control protein (CCP) modules reveals mobility in binding surfaces. Protein Sci 2004;13:1238–50.
5. Soares DC, Gerloff DL, Syme NR, Coulson AF, Parkinson J, Barlow PN. Large-scale modelling as a route to multiple surface comparisons of the CCP module family. Protein Eng Des Sel 2005;18:379–88.
6. Meindl A, Carvalho MR, Herrmann K, Lorenz B, Achatz H, Apfelstedt-Sylla E, Wittwer B, Ross M, Meitinger T. A gene (SRPX) encoding a sushi-repeat-containing protein is deleted in patients with X-linked retinitis pigmentosa. Hum Mol Genet 1995;4:2339–46.
7. Dry KL, Aldred MA, Edgar AJ, Brown J, Manson FD, Ho MF, Prosser J, Hardwick LJ, Lennon AA, Thomson K, Keuren MV, Kumit DM, et al. Identification of a novel gene, ETX1 from Xp21.1, a candidate gene for X-linked retintis pigmentosa (RP3). Hum Mol Genet 1995;4:2347–53.
8. Callebaut I, Gilges D, Vigon I, Mornon JP. HYR, an extracellular module involved in cellular adhesion and related to the immunoglobulin-like fold. Protein Sci 2000;9:1382–90.
9. Yamada Y, Arao T, Gotoda T, Taniguchi H, Oda I, Shirao K, Shimada Y, Hamaguchi T, Kato K, Hamano T, Koizumi F, Tamura T, et al. Identification of prognostic biomarkers in gastric cancer using endoscopic biopsy samples. Cancer Sci 2008;99:2193–99.
10. Yamanaka R, Arao T, Yajima N, Tsuchiya N, Homma J, Tanaka R, Sano M, Oide A, Sekijima M, Nishio K. Identification of expressed genes characterizing long-term survival in malignant glioma patients. Oncogene 2006;25:5994–6002.
11. Parsons JT. Focal adhesion kinase: the first ten years. J Cell Sci 2003; 116:1409–16.
12. Pala D, Kapoor M, Woods A, Kennedy L, Liu S, Chen S, Bursell L, Lyons KM, Carter DE, Beier F, Leask A. Focal adhesion kinase/Src suppresses early chondrogenesis: central role of CCN2. J Biol Chem 2008;283:9239–47.
13. Lan CC, Wu CS, Chiou MH, Hsieh PC, Yu HS. Low-energy helium-neon laser induces locomotion of the immature melanoblasts and promotes melanogenesis of the more differentiated melanoblasts: recapitulation of vitiligo repigmentation in vitro. J Invest Dermatol 2006; 126:2119–26.
14. Mousa SA. Cell adhesion molecules: potential therapeutic & diagnostic implications. Mol Biotechnol 2008;38:33–40.
15. Vestweber D, Blanks JE. Mechanisms that regulate the function of the selectins and their ligands. Physiol Rev 1999;79:181–213.
16. Mineur P, Guignandon A, Lambert ChA, Amblard M, Lapiere ChM, Nusgens BV. RGDS and DGEA-induced [Ca2+]i signalling in human dermal fibroblasts. Biochim Biophys Acta 2005;1746:28–37.
17. Schaller MD. FAK and paxillin: regulators of N-cadherin adhesion and inhibitors of cell migration? J Cell Biol 2004;166:157–9.
18. Mitra SK, Schlaepfer DD. Integrin-regulated FAK-Src signaling in normal and cancer cells. Curr Opin Cell Biol 2006;18:516–23.
19. Royer-Zemmour B, Ponsole-Lenfant M, Gara H, Roll P, Leveque C, Massacrier A, Ferracci G, Cillario J, Robaglia-Schlupp A, Vincentelli R, Cau P, Szepetowski P. Epileptic and developmental disorders of the speech cortex: ligand/receptor interaction of wild-type and mutant SRPX2 with the plasminogen activator receptor uPAR. Hum Mol Genet 2008;17:3617–30.
20. Witz IP. The selectin-selectin ligand axis in tumor progression. Cancer Metastasis Rev 2008;27:19–30.
21. Barthel SR, Gavino JD, Descheny L, Dimitroff CJ. Targeting selectins and selectin ligands in inflammation and cancer. Expert Opin Ther Targets 2007;11:1473–91.
22. Oh IY, Yoon CH, Hur J, Kim JH, Kim TY, Lee CS, Park KW, Chae IH, Oh BH, Park YB, Kim HS. Involvement of E-selectin in recruitment of endothelial progenitor cells and angiogenesis in ischemic muscle. Blood 2007;110:3891–9.
23. Egami K, Murohara T, Aoki M, Matsuishi T. Ischemia-induced angiogenesis: role of inflammatory response mediated by P-selectin. J Leukoc Biol 2006;79:971–6.
24. Hunger SP. Chromosomal translocations involving the E2A gene in acute lymphoblastic leukemia: clinical features and molecular pathogenesis. Blood 1996;87:1211–24.

Oncogene (2009) 28, 518–533
© 2009 Macmillan Publishers Limited All rights reserved 0950-9232/09 $32.00
www.nature.com/onc

ORIGINAL ARTICLE

Disruption of the EGFR E884–R958 ion pair conserved in the human kinome differentially alters signaling and inhibitor sensitivity

Z Tang[1], S Jiang[1], R Du[1], ET Petri[2], A El-Telbany[1], PSO Chan[3], T Kijima[4], S Dietrich[1], K Matsui[5], M Kobayashi[5], S Sasada[5], N Okamoto[5], H Suzuki[5], K Kawahara[6], T Iwasaki[7], K Nakagawa[7], I Kawase[4], JG Christensen[8], T Hirashima[5], B Halmos[1], R Salgia[9], TJ Boggon[2], JA Kern[10] and PC Ma[1]

[1]Division of Hematology/Oncology, Case Western Reserve University School of Medicine, University Hospitals Case Medical Center and Ireland Cancer Center, Case Comprehensive Cancer Center, Cleveland, OH, USA; [2]Department of Pharmacology, Yale University School of Medicine, New Haven, CT, USA; [3]Elpidex Bioscience Inc., Los Angeles, CA, USA; [4]Department of Respiratory Medicine, Allergy and Rheumatic Diseases, Osaka University Graduate School of Medicine, Osaka, Japan; [5]Department of Thoracic Malignancy, Osaka Prefectural Medical Center for Respiratory and Allergic Disease, Osaka, Japan; [6]Department of Pathology, Osaka Prefectural Medical Center for Respiratory and Allergic Disease, Osaka, Japan; [7]Department of Thoracic Surgery, Osaka Prefectural Medical Center for Respiratory and Allergic Disease, Osaka, Japan; [8]Pfizer Inc., Global Research and Development, San Diego, CA, USA; [9]Section of Hematology/Oncology, University of Chicago Pritzker School of Medicine, University of Chicago Cancer Research Center, Chicago, IL, USA and [10]Division of Pulmonary, Critical Care and Sleep Medicine, Case Western Reserve University School of Medicine, University Hospitals Case Medical Center and Ireland Cancer Center, Case Comprehensive Cancer Center, Cleveland, OH, USA

Targeted therapy against epidermal growth factor receptor (EGFR) represents a major therapeutic advance in lung cancer treatment. Somatic mutations of the *EGFR* gene, most commonly L858R (exon 21) and short in-frame exon 19 deletions, have been found to confer enhanced sensitivity toward the inhibitors gefitinib and erlotinib. We have recently identified an EGFR mutation E884K, in combination with L858R, in a patient with advanced lung cancer who progressed on erlotinib maintenance therapy, and subsequently had leptomeningeal metastases that responded to gefitinib. The somatic E884K substitution appears to be relatively infrequent and resulted in a mutant lysine residue that disrupts an ion pair with residue R958 in the EGFR kinase domain C-lobe, an interaction that is highly conserved within the human kinome as demonstrated by our sequence analysis and structure analysis. Our studies here, using COS-7 transfection model system, show that E884K works in concert with L858R in-*cis*, in a dominant manner, to change downstream signaling, differentially induce Mitogen-activated protein kinase (extracellular signaling-regulated kinase 1/2) signaling and associated cell proliferation and differentially alter sensitivity of EGFR phosphorylation inhibition by ERBB family inhibitors in an inhibitor-specific manner. Mutations of the conserved ion pair E884–R958 may result in conformational changes that alter kinase substrate recognition. The analogous E1271K-MET mutation conferred differential sensitivity toward preclinical MET inhibitors SU11274 (unchanged) and PHA665752 (more sensitive). Systematic bioinformatics analysis of the mutation catalog in the human kinome revealed the presence of cancer-associated mutations involving the conserved E884 homologous residue, and adjacent residues at the ion pair, in known proto-oncogenes (*KIT*, *RET*, *MET* and *FAK*) and tumor-suppressor gene (*LKB1*). Targeted therapy using small-molecule inhibitors should take into account potential cooperative effects of multiple kinase mutations, and their specific effects on downstream signaling and inhibitor sensitivity. Improved efficacy of targeted kinase inhibitors may be achieved by targeting the dominant activating mutations present.

Oncogene (2009) **28**, 518–533; doi:10.1038/onc.2008.411; published online 17 November 2008

Keywords: *EGFR*; *MET*; mutation; tyrosine kinase inhibitor; structure; kinome

Correspondence: Dr PC Ma, Division of Hematology/Oncology, Case Western Reserve University School of Medicine, University Hospitals Case Medical Center and Ireland Cancer Center, Case Comprehensive Cancer Center, 10900 Euclid Avenue, WRB 2-123, Cleveland, OH 44106, USA.
E-mail: patrick.ma@case.edu
Received 10 March 2008; revised 17 September 2008; accepted 1 October 2008; published online 17 November 2008

Introduction

Targeted therapy using epidermal growth factor receptor (EGFR) kinase inhibitors represents a major therapeutic advance in lung cancer treatment. Somatic mutations of the *EGFR* gene, most commonly L858R (exon 21) and short in-frame deletions in exon 19, have recently been identified as catalytic domain mutation hotspots (Shigematsu and Gazdar, 2006). These mutations confer enhanced sensitivity toward the anilinoquinazoline kinase inhibitors gefitinib and erlotinib (Lynch *et al.*, 2004;

Paez *et al.*, 2004). A mutation conferring resistance to these two kinase inhibitors, T790M (exon 20), has also been found in the EGFR kinase domain and can account for about half of the cases of acquired resistance (Kobayashi *et al.*, 2005). There are a number of other kinase domain mutations of EGFR that occur at lower frequencies, most often in combination with L858R (Tam *et al.*, 2006). However, how these mutations might interact when present together in-*cis* is unknown.

We recently identified a novel EGFR kinase domain somatic mutation, E884K (Glu884Lys, exon 22) in a patient with stage IV non-small-cell lung cancer, in combination with the L858R mutation (L858R + E884K) (Choong *et al.*, 2006). The patient initially received carboplatin/paclitaxel and erlotinib and then developed brain metastasis on maintenance erlotinib. In spite of further treatment with whole brain radiation, temozolomide and irinotecan, the patient's disease progressed to symptomatic leptomeningeal carcinomatosis, which responded to gefitinib, a year after being off an EGFR kinase inhibitor. The L858R + E884K double mutation was found both in her pretreatment diagnostic thoracic lymph node biopsy specimen as well as in the tumor cells (extracted by laser microdissection) within the cerebrospinal fluid during the course of leptomeningeal metastases (Choong *et al.*, 2006). The E884K mutation represents the first mutation reported to show an apparent differential response to the two EGFR kinase inhibitors erlotinib and gefitinib, whereas L858R was known to be sensitizing to both. These findings led to our hypothesis that EGFR kinase mutations can work together to differentially alter inhibitor sensitivity and downstream signaling. Further biochemical analysis in our current study indicates that the double mutant EGFR (L858R + E884K) responds differently to gefitinib and erlotinib. We now show that E884K works in concert with L858R, and in a dominant manner, to mediate differential sensitivity to kinase inhibitors through altered phosphorylation of AKT and signal transducer and activator of transcription 3 (STAT3) and were correlated with differential cellular cytotoxicity and induction of the apoptotic marker cleaved-PARP(Asp214) by EGFR inhibitors. Using a combination of bioinformatics and structural analyses, we further characterized the role of the E884 residue in EGFR kinase function. Our results further demonstrate that the ion pair formed by residues E884 and R958 in the EGFR kinase domain is a highly conserved feature of protein kinases in the human kinome, including many 'druggable' targets such as MET. Disruption of the conserved ion pair in EGFR modulates downstream signal transduction and differentially alters kinase inhibitor sensitivity in an inhibitor-specific manner.

Results

E884K works in concert with L858R mutation to confer differential inhibitor sensitivity through inhibition of AKT and STAT3 downstream signaling

We hypothesize that EGFR kinase mutations can work together to differentially alter inhibitor sensitivity. To test this hypothesis, *EGFR* expression constructs engineered with L858R (LR) or dual mutations of L858R + E884K (LR + EK) were stably transfected into COS-7 cells. Cells were treated with increasing concentrations of either erlotinib or gefitinib in the presence of EGF stimulation (Figure 1a). Compared with L858R alone, the L858R + E884K dual mutant was less sensitive to erlotinib in the inhibition of tyrosine phosphorylation of EGFR. Conversely, E884K worked in concert with L858R in-*cis* to further enhance the sensitivity of the mutant receptor to gefitinib inhibition (Figures 1a and b). These findings correlated with the clinical course of the patient's response profile (Choong *et al.*, 2006) and highlight the potential for EGFR kinase mutations to exert concerted effects in-*cis* to impact targeted inhibition.

To gain insight into the mechanism of E884K modulation of EGFR tyrosine kinase inhibitor (TKI) sensitivity, we further studied its effect on downstream AKT and STAT3 signaling pathways with TKI inhibition. The effect on the downstream signal mediators p-AKT (S473) and p-STAT3 (Y705) correlated well with the inhibition of EGFR phosphorylation (Figure 1a); E884K in-*cis* with L858R decreased erlotinib inhibition of AKT and STAT3 phosphorylation but increased inhibition by gefitinib. The differential inhibition exerted by E884K on EGFR, AKT and STAT3 signaling also corresponded to the inhibitor-induced expression pattern of the apoptotic marker, cleaved-PARP(Asp214) (Figure 1c). Similarly, there was an opposite effect of the E884K mutation over L858R in-*cis* in inducing cellular cytotoxicity by erlotinib and gefitinib (Figure 1d). Hence, E884K in-*cis* with L858R differentially altered inhibitor sensitivity when compared with L858R alone, through differential inhibition of the prosurvival AKT and STAT3 signaling pathways associated with altered induction of cleaved-PARP(Asp214).

E884K-EGFR modulates inhibitor sensitivity effects in an inhibitor-specific manner

To further examine the hypothesis that EGFR mutations exert effects in combination that are unique to a specific kinase inhibitor, we further tested the mutant EGFR expressing L858R alone or L858R + E884K in-*cis*, against several other ERBB family TKIs, including both reversible inhibitors (4557W, Lapatinib, GW583340, Tyrphostin-AG1478) and irreversible inhibitor (CL-387,785) (Figure 2 and Supplementary Figure 2). We focused on the effects of these inhibitors on the sensitivity of inhibition of the EGFR kinase phosphorylation in the mutant EGFR. As the tyrosine phosphorylation of the EGFR has been shown to correlate well with its catalytic enzymatic activity, we used the tyrosine phosphorylation of the pY1068 (GRB1-binding site) epitope of EGFR as the surrogate measurement of the extent of inhibition by the TKIs. For 4557W (reversible dual TKI of EGFR/ERBB2), the E884K mutation modulated the L858R mutation in-*cis*, again in a dominant manner, rendering the double-mutant receptor more sensitive to the dual inhibitor

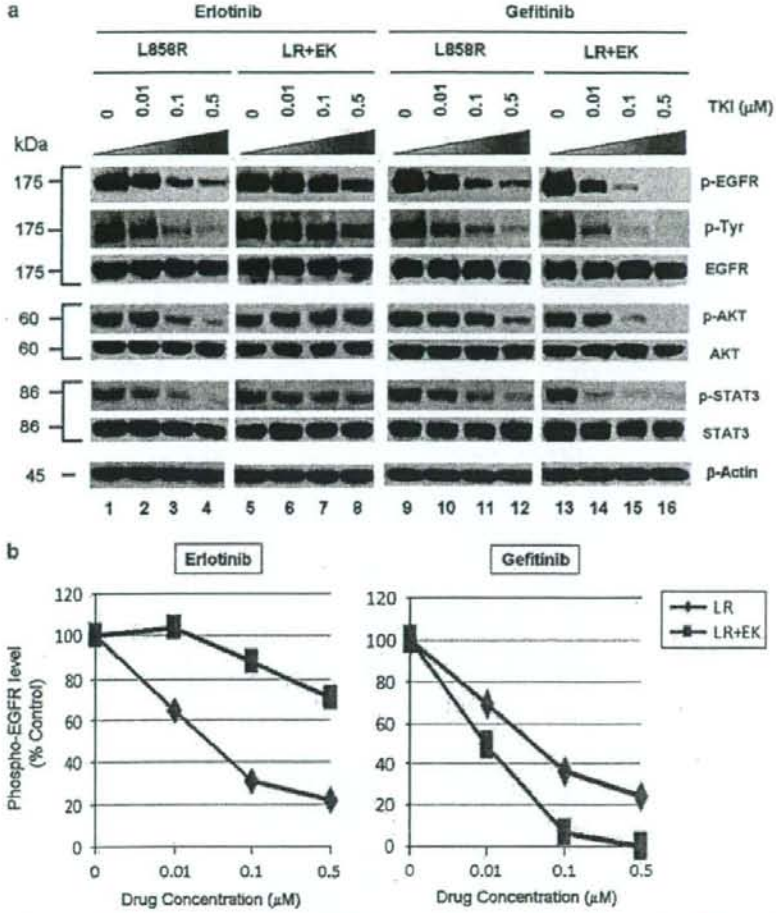

Figure 1 E884K mutation of epidermal growth factor receptor (EGFR) worked in concert with L858R to differentially alter sensitivity to EGFR kinase inhibitors erlotinib and gefitinib. (**a**) Stable COS-7 transfects expressing the L858R and double-mutant L858R + E884K variants of *EGFR* were used in the experiment. The endogenous wild-type EGFR expression of parental COS-7 cells is negligible (data not shown). Cells were cultured in 0.5% bovine serum albumin-containing serum-free media for 16 h and then incubated with increasing concentrations of either erlotinib or gefitinib in the presence of EGF (100 ng/ml). Whole-cell lysates were extracted for SDS polyacrylamide gel electrophoresis and immunoblotting using antibodies against: p-EGFR (Y1068), phosphotyrosine (p-Tyr), EGFR, p-AKT (S473), AKT, p-STAT3 (Y705), STAT3 and β-actin. The experiment was performed in duplicate with reproducible results. The E884K mutation negatively modulated the effect of L858R to erlotinib inhibition in a dominant manner but enhanced sensitivity of the mutant receptor to gefitinib inhibition. (**b**) Densitometric quantitation of the p-EGFR (Y1068) levels showing differential alteration of sensitivity to erlotinib (more resistant) and gefitinib (more sensitive) by the E884K mutation when in-*cis* with L858R. The densitometric scanning of the p-EGFR immunoblot bands was performed digitally using the NIH ImageJ software program and was normalized to the total EGFR expression levels. (**c**) Relative expression of the apoptotic marker cleaved-PARP(Asp214) in L858R and L858R + E884K *EGFR* variants treated with increasing concentrations of erlotinib (left) and gefitinib (right). The immunoblot from whole cell lysates as in (**a**), using anti-cleaved-PARP(Asp214) (c-PARP) antibody is shown here (above) together with the densitometric quantitation (below) adjusted to β-actin loading control using the NIH ImageJ software program. (**d**) COS-7 cells with stable transduced expression of L858R or L858R + E884K mutant *EGFR* were tested in cellular cytotoxicity assay *in vitro* under drug treatment with either erlotinib or gefitinib at indicated concentrations. Results are shown in percentage change of cell viability of L858R + E884K EGFR-COS-7 compared with the control L858R EGFR-COS-7 cells at each concentration of TKI tested. E884K mutation, when in-*cis* with L858R, significantly decreased the sensitivity of cell viability inhibition by erlotinib compared with L858R alone; however, it significantly increased the sensitivity of cell viability inhibition by gefitinib compared with L858R alone. In the case of erlotinib, E884K was desensitizing to L858R, leading to lower cytotoxicity (56.3 ± 2.68% increased viable cells after inhibition at 5 μM, $P = 0.0004$) compared with L858R alone. Conversely, in gefitinib inhibition, E884K further sensitized L858R in-*cis*, leading to significantly higher cytotoxicity (63.5 ± 6.86% decreased viable cells after inhibition at 5 μM, $P = 0.0013$) compared with L858R alone. Error bar, s.d. ($N = 3$). $^*P < 0.05$, compared with L858R alone. Representative photomicrographs of cells after 48 h of indicated inhibitor treatment (5 μM) *in vitro* were included to illustrate the presence of differential cytotoxicity as seen with the nonviable detached cells or cell fragments (× 10). Examples of increased floating nonviable cells are highlighted with arrows.

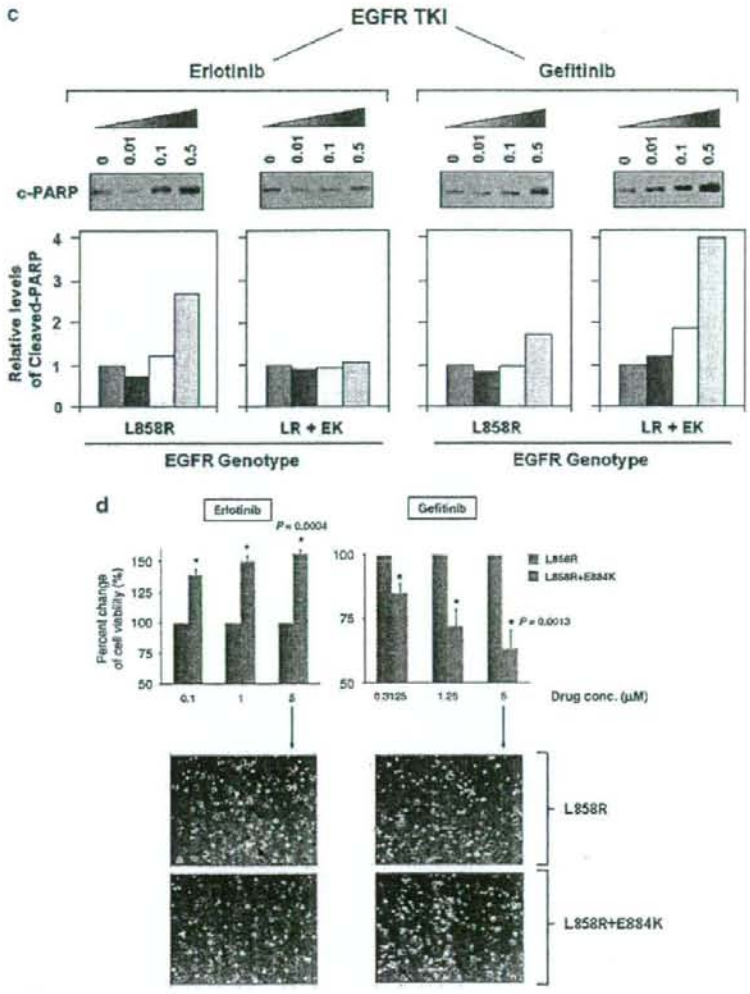

Figure 1 Continued.

(Figure 2). Hence, E884K mutation can work in concert with L858R to modulate mutant receptor sensitivity to different targeted inhibitors. Similarly, E884K further enhanced the sensitivity of L858R to the inhibition by the irreversible EGFR/ERBB2 inhibitor, CL-387,785. On the other hand, the sensitivity of EGFR phosphorylation between the L858R and L858R + E884K EGFR receptors in Tyrphostin-AG1478 (reversible EGFR-TKI), GW583340 (reversible dual EGFR/ERBB2-TKI) and lapatinib (reversible dual EGFR/ERBB2-TKI) did not significantly differ. Hence, the E884K mutation, when in-*cis* with L858R, modulates the sensitivity of the mutant receptor toward ERBB family kinase inhibitors in an inhibitor-specific manner.

E884K is activating, and can work cooperatively with L858R to differentially modulate downstream signal transduction

To address the question whether there are other downstream phosphoproteins that can be differentially activated by the E884K mutation compared with the activating L858R mutation, the global phosphotyrosine profiles of the cellular proteins induced by the mutant EGFR were examined. The E884K alone and L858R + E884K double-mutant EGFR remained sensitive to EGF, and the E884K mutation cooperates with L858R when in-*cis* to further enhance the mutational effects on downstream phosphoprotein activation (data not shown). To date, essentially all mutational combinations involving L858R studied thus far were found to

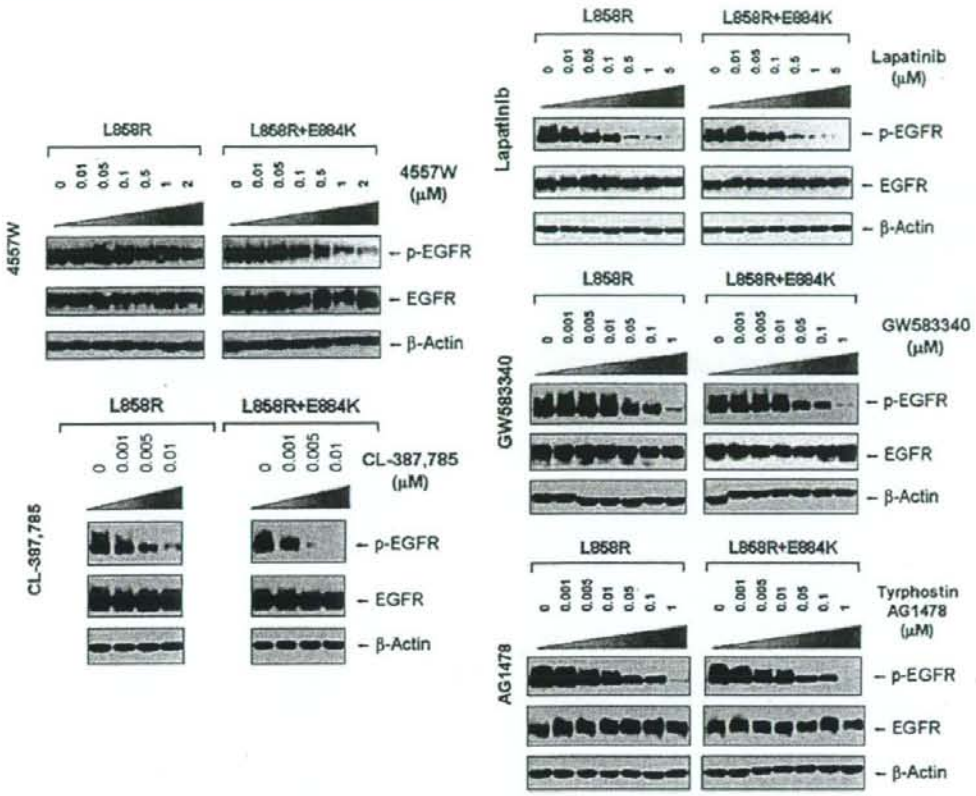

Figure 2 Effects of L858R/E884K-EGFR on other epidermal growth factor receptor (EGFR) kinase inhibitors. The EGFR mutation E884K modulated L858R mutation in-*cis* with inhibitor-specific effects on the sensitivities to EGFR phosphorylation inhibition by the inhibitors (4557W, GW583340, Tyrphostin-AG1478, lapatinib and CL-387,785). Stable COS-7 transfectant cells expressing equivalent levels of the following *EGFR* variants were used: L858R (LR) and L858R + E994K (LR + EK). Cells were cultured in 0.5% bovine serum albumin-containing serum-free media for 16 h, and then treated with or without increasing concentrations of the EGFR TKIs as indicated, in the presence of EGF stimulation (100 ng/ml). Whole cell lysates were extracted for SDS polyacrylamide gel electrophoresis and immunoblotting using the following antibodies: p-EGFR (Y1068), EGFR and β-actin. E884K mutation worked in concert with L858R in-*cis* to enhance the sensitivity of the mutant receptor to inhibition by the kinase inhibitor 4557W, and CL-387,785. On the other hand, it has little effects on the inhibition by lapatinib, GW583340 and Tyrphostin-AG1478.

exist in-*cis*, suggesting potential *cis* mutation-to-mutation cooperation in EGFR signaling and possibly tumorigenesis (Tam *et al*., 2006). To determine the effect of E884K on mutant EGFR signaling, we next studied the EGFR activation of the downstream PI3K-AKT-MAPK (ERK1/2)-STAT pathway. E884K mutant (alone or in-*cis* with L858R) receptor exhibited constitutive activation of the tyrosine phosphorylated EGFR comparable with L858R (Figure 3a). E884K and L858R + E884K mutants remained sensitive to EGF and were activated by the ligand to a level comparable with L858R (Figure 3a). L858R was associated with downstream activation of p-AKT signaling, which was inducible by EGF stimulation. When in-*cis* with L858R, E884K mutation (L858R + E884K) downregulated constitutive AKT phosphorylation. E884K, alone or in-*cis* with L858R, can also mediate constitutive induction of p-STAT3 (pY705) (important for STAT3 dimerization and transcriptional activation of target genes) (Figure 3a). Interestingly, the double mutation L858R + E884K conferred a distinctly more sensitive response to EGF stimulation selectively in the mitogen-activated protein kinase (extracellular signaling-regulated kinase 1/2) (MAPK-ERK1/2) cell proliferation pathway compared with either wild type, E884K alone or L858R alone. Consistent with this differential signaling effect, the L858R + E884K-COS-7 cells had a significantly higher cell proliferation rate than that of the L858R-COS-7 cells in the MTS cell proliferation assay for 5 days (Figure 3b). At days 3 and 5, the cell proliferation rate as determined by % viable cell increase during the assay period was 1.46-fold (day 3) and 1.40-fold ($P = 0.0013$) higher (day 5) in L858R + E884K than L858R alone. L858R + E884K

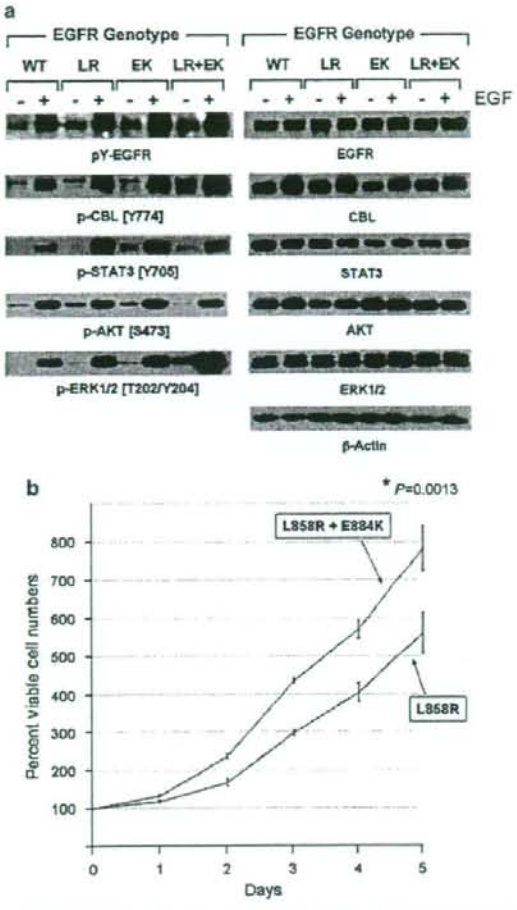

Figure 3 Effects of mutational disruption of the Glu(E)884 Arg(R)958 ion pair in epidermal growth factor receptor (EGFR) signaling. (**a**) Stable COS-7 transfectant cells expressing the various *EGFR* variants were cultured in 0.5% bovine serum albumin-containing serum-free media, followed by EGF stimulation (100 ng/ml, 10 min). Whole cell lysates were prepared for SDS polyacrylamide gel electrophoresis and immunoblotted using the antibodies against: phosphotyrosine (pY-EGFR), EGFR, p-CBL (Y774), CBL, p-STAT3 (Y705), STAT3, p-AKT (S473), AKT, p-ERK1/2 (T202/Y204), ERK1/2 and β-actin. E884K, either alone or in-*cis* with L858R, modulated differential activation of downstream mutant EGFR signaling. (**b**) The EGFR double mutations L858R + E884K conferred a significantly higher cell proliferation rate than L858R alone in the COS-7 cells stably expressing the transduced mutant *EGFR*. Cellular viability assay was performed with the cells growing in regular growth media (10% fetal bovine serum) up to 5 days as described in Materials and methods. The MTS viability assay was performed in triplicate. Error bar, s.d. $^*P = 0.0013$.

also conferred a higher induction of p-CBL as well. Hence, the double mutation L858R + E884K modulated basal and stimulated downstream EGFR signaling differentially with differential effects on the AKT (downregulated), CBL and MAPK-ERK1/2 phosphorylation (upregulated). Moreover, E884K had a dominant effect over L858R, when in-*cis*, in these signaling modulatory effects.

Disruption of a conserved ion pair, Glu(E)884-Arg(R)958, in EGFR differentially alters kinase inhibitor sensitivity

Next, bioinformatics analysis of the E884 residue was performed by multiple kinase domain amino-acid sequence alignments of the human kinome, using the AliBee multiple sequence alignment program (GeneBee, Moscow, Russia) (Supplementary Figure 1). Amino-acid alignments of the kinase domains of phylogenetically diverse groups of kinases such as among the ERBB family, the vascular endothelial growth factor receptor family and the TRK family show that the E884 residue is highly conserved (Figure 4a). In addition, a second residue was also found to be highly conserved (R958) (Figure 4a). Further multiple sequence alignments of 321 human kinase domains show high conservation of both E884 and R958 residues of the EGFR kinase domain (Supplementary Figure 1). The glutamic acid residue (E884) is conserved in >77% and the arginine residue (R958) is conserved in >55% of human kinases in the kinome.

Finally, we mapped the locations of the L858R and E884K mutations onto the three-dimensional structure of the EGFR kinase domain complexed with erlotinib and with lapatinib (PDB accession codes 1M17 (Stamos *et al*., 2002) and 1XKK (Wood *et al*., 2004)) (Figure 4b). We also generated a superposition of the EGFR kinase domain with multiple diverse kinase catalytic domains (Figure 4c). These analyses show the structural conservation of the buried Glu(E)-Arg(R) ion pair and that the exon 22 residue, E884, is physically distant from L858 in exon 21. Furthermore, unlike L858, E884 is not proximal to the adenosine triphosphate-binding cleft of the kinase domain, making it difficult to predict its effects on kinase inhibitor interactions. Mutation of the acidic glutamate residue at codon 884 to a basic lysine will disrupt the highly conserved ion pair through charge–charge repulsion with the basic residue R958 (Figures 4b and c).

To further test the hypothesis of the disruption of the conserved E884–R958 salt bridge as a mechanism underlying the differential response of the mutant EGFR to kinase inhibitors, we tested the double mutant L858R + R958D against erlotinib and gefitinib (Figure 5). Substitution of the wild-type Arg(R)958 with Asp(D)958 was created using site-directed mutagenesis. We hypothesized that the R958D substitution would disrupt the ion pair with E884 through electrostatic repulsion, in a way similar to the effect of the E884K substitution. COS-7 cells transfected to express the indicated mutant EGFR receptors were inhibited using either erlotinib or gefitinib *in vitro* with increasing concentrations. Similar to E884K, R958D modulated the sensitizing effect of L858R differentially to reversible EGFR inhibitors when in-*cis* (with L858R). R958D mutation, when in-*cis* with L858R, decreased the

sensitivity of the mutant receptor to erlotinib inhibition, while increasing the sensitivity to gefitinib in a dominant manner (Figures 5a and b).

Mutational disruption of the conserved kinase ion pair in MET kinase by E1271K-MET also differentially alters the sensitivity of phosphorylation inhibition by MET inhibitors

MET has been shown to play a key role in the development of many human malignancies. A number of mutations have been identified in *MET* from various cancers. Recently, it has been shown that MET represents a key oncogenic signaling in lung cancer alongside with EGFR signaling (Rikova *et al.*, 2007; Guo *et al.*, 2008; Tang *et al.*, 2008). Moreover, MET can cross-activate with EGFR when they are co-expressed, which happens rather frequently (Rikova *et al.*, 2007; Tang *et al.*, 2008). MET has also been shown to be an attractive therapeutic molecular target (Ma *et al.*, 2003b; Shinomiya *et al.*, 2004; Mazzone and Comoglio, 2006; Peruzzi and Bottaro, 2006; Smolen *et al.*, 2006). Here, we test the hypothesis that E1271K mutation of *MET*, analogous to E884K-*EGFR*, can also differentially alter inhibitory sensitivity toward selective MET inhibitors (Figure 6). The Glu(E)1271-Arg(R)1345 constitutes the conversed ion-pair in MET kinase (Figures 4 and 6). The location of the E1271–R1234 ion pair in MET kinase is illustrated in the recently reported crystallographic structure of the MET kinase domain complexed with SU11274 (Bellon *et al.*,

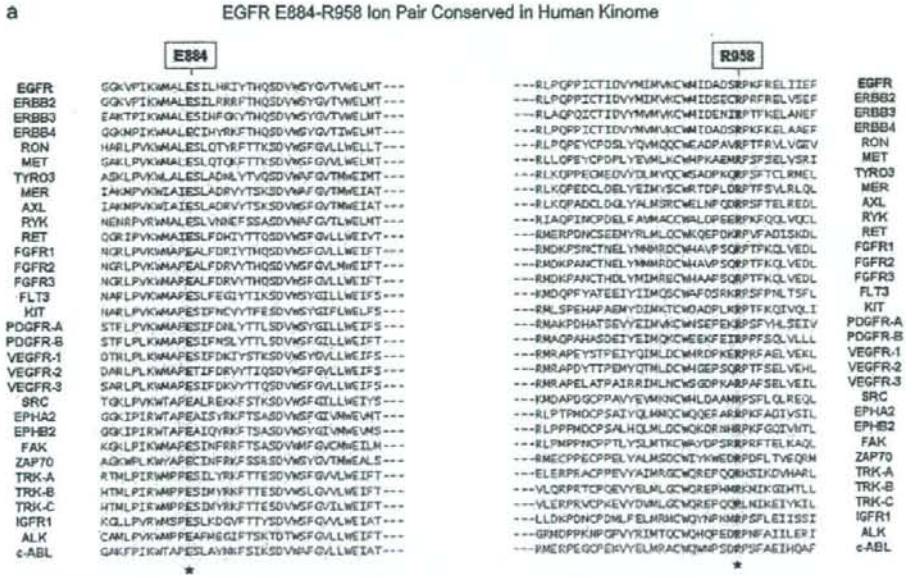

Figure 4 The ion pair Glu(E)884-Arg(R)958 in the epidermal growth factor receptor (EGFR) kinase domain is a highly conserved feature in the human kinome. (**a**) A selected list of 32 diverse human protein kinases with known importance as validated or potential cancer therapeutic targets was included here with bioinformatics alignment analysis of the kinase domain amino-acid sequences. Glu884 (E884) and Arg958 (R958) of EGFR are both highly conserved residues among these kinases. (Left) Amino-acid alignment of the kinase domains of 32 diverse members of human protein kinases showing E884-EGFR is highly conserved: EGFR, ERBB2, ERBB3, ERBB4, RON, MET, TYRO3, MER, AXL, RYK, RET, FGFR1, FGFR2, FGFR3, FLT3, KIT, PDGFR-A, PDGFR-B, vascular endothelial growth factor receptor-1, vascular endothelial growth factor receptor-2, vascular endothelial growth factor receptor-3, SRC, EPHA2, EPHB2, FAK, ZAP70, TRK-A, TRK-B, TRK-C, IGFR1, ALK and c-ABL. (Right) R958-EGFR is also highly conserved among diverse members of kinases. For the complete alignment analysis of kinase domains of the human kinome, see Supplementary Figure 1. (**b**) EGFR kinase domain crystal structures (PDB accession codes 1M17 (Stamos *et al.*, 2002) and 1XKK (Wood *et al.*, 2004)) when in complex with erlotinib (blue) and lapatinib (green) are shown. The locations of L858 (exon 21) and E884 (exon 22) are highlighted. E884 (acidic) and R958 (basic) residues form an ion pair in wild-type EGFR that would be disrupted by the E884K substitution from the acidic glutamic acid (E) to the basic lysine (K). The E884 R958 salt bridge is present in the kinase domain crystal structures complexed to either erlotinib or lapatinib. (**c**) Superposition of the EGFR kinase domain with the catalytic domains of diverse kinases shows structural conservation of a buried Glu(E) Arg(R) ion pair. The crystal structure of EGFR tyrosine kinase (PDB accession code: 1M17) (Stamos *et al.*, 2002) was superimposed with the catalytic kinase domains of human CDK2 (PDB accession code: 1VYW) (Pevarello *et al.*, 2004), human JNK3 (PDB accession code: 1PMQ) (Scapin *et al.*, 2003), human insulin receptor kinase (PDB accession code: 1IR3) (Hubbard, 1997), ZAP-70 tyrosine kinase (PDB accession code: 1U59) (Jin *et al.*, 2004), LCK kinase (PDB accession code: 1QPD) (Zhu *et al.*, 1999) and MET (PDB accession code: 2RFS) (Bellon *et al.*, 2008) using Cα atoms in the program DeepView/Swiss-PdbViewer v3.7. The conserved Glu Arg ion pair is shown in stick format, with oxygen atoms colored red and nitrogens, blue. The EGFR side chains are shown in yellow. The structural location of the ion pair is conserved in these crystal structures and helps orientate helix αEF. Figures 4b and c were prepared using the program PYMOL (www.pymol.org).

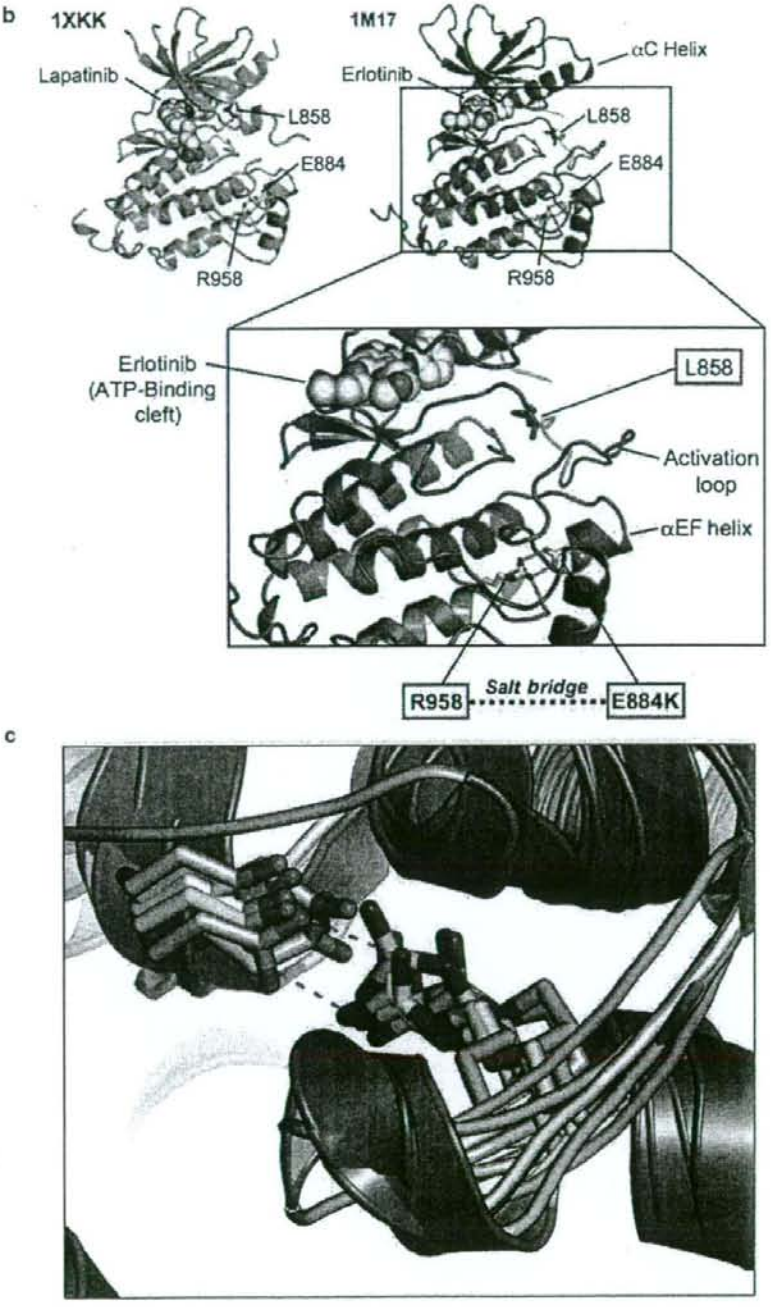

Figure 4 Continued.

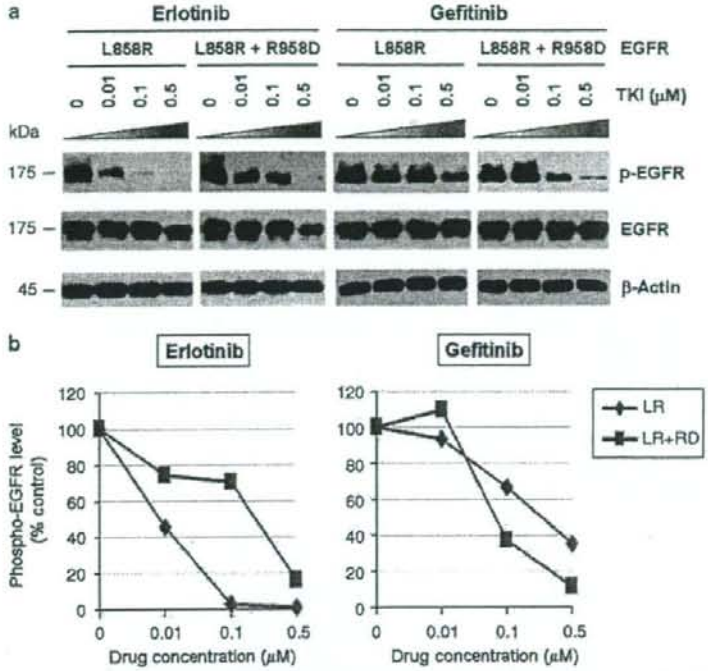

Figure 5 Disruption of the conserved Glu(E)884 Arg(R)958 salt bridge by a R958D substitution differentially altered L858R mutant receptor sensitivity to epidermal growth factor receptor (EGFR) inhibitors. (a) Stable COS-7 transfects expressing the sensitizing L858R and double-mutant L858R + R958D variants of EGFR were cultured in 0.5% bovine serum albumin-containing serum-free media for 16 h, and then incubated with increasing concentrations of either erlotinib or gefitinib, in the presence of EGF stimulation (100 ng/ml). Whole-cell lysates were extracted for SDS polyacrylamide gel electrophoresis and immunoblotted using antibodies against the followings: p-EGFR (Y1068), EGFR and β-actin. R958D mutation modulated the effect of L858R on inhibitor sensitivity resulting in desensitization of the mutant receptor to erlotinib inhibition but modestly enhanced sensitivity to gefitinib inhibition. (b) Densitometric quantitation of the p-EGFR (Y1068) levels showing that R958D mutation differentially altered L858R mutant receptor sensitivity to erlotinib (more resistant) and gefitinib (more sensitive). Densitometric scanning of the immunoblot signals shown in (a) was performed using NIH ImageJ software program, with normalization to total EGFR expression levels.

2008). Stable COS-7 transfectant cells expressing similar levels of wild type and E1271K-*MET* were used in this experiment using the two reversible preclinical MET inhibitors SU11274 (Ma *et al.*, 2005a) and PHA665752 (Ma *et al.*, 2005a, b). We did not find any significant modulation of sensitivity to SU11274 inhibition in the E1271K-MET cells (Figure 6b). On the other hand, the E1271K mutation of MET enhanced the sensitivity of inhibition by PHA665752 in the phosphorylation of the mutant MET at its major autophosphorylation sites (pY1234/1235) (equivalent to pY1252/1253 phosphosites as in the full-length *MET* transcript, with a difference of 18 amino acids in the exon 10 with the common alternatively spliced variant) in the kinase domain, and its downstream signaling proteins AKT and ERK1/2 (Figure 6b). Hence, disrupting the MET kinase salt bridge by the E1271K mutation also differentially alters sensitivity to MET kinase inhibitors in an inhibitor-specific manner.

Mutations at the conserved Glu(E)–Arg(R) ion pair in the human kinome

As the E884K somatic mutation was originally identified in a never-smoker woman of Japanese descent, we performed mutational screening for the presence of mutation at the E884 and R958 residues of *EGFR* among a cohort of 67 lung tumor genomic DNA specimens from Japanese non-small-cell lung cancer patients (including 66 transbronchial biopsies and 1 surgical specimen). Nonsynonymous mutations were not present in either residue location in this patient cohort. On the basis of our results suggesting the conserved structure and function of the Glu(E)–Arg(R) ion pair in EGFR and among other kinases in the kinome, we hypothesized that there would be other cancer-associated mutations at the conserved ion pair within the human kinome in kinases other than EGFR. Here, we performed bioinformatics survey of the updated Catalog of Somatic Mutations In Cancer (COSMIC) database (http://www.sanger.ac.uk/genetics/CGP/cosmic/) containing

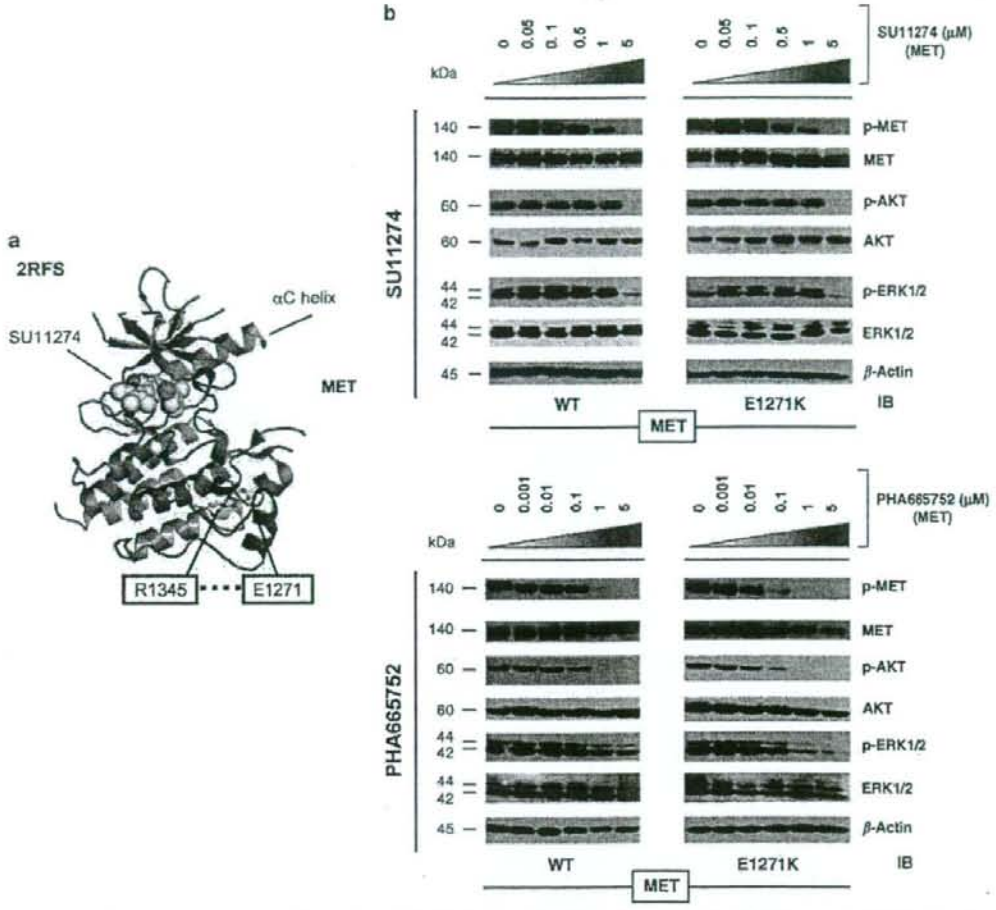

Figure 6 Mutational disruption of the conserved E1271 R1345 ion pair in MET kinase salt bridge causes inhibitor-specific modulation of sensitivity to SU11274 (unchanged) and PHA665752 (more sensitive). (a) MET kinase domain crystal structure (PDB accession code: 2RFS) (Bellon *et al*., 2008) highlighting the salt bridge between E1271 and R1345. Crystal structure solved in complex with SU11274 is shown. The conserved Glu Arg ion pair is shown in stick format, with oxygen atoms colored red, nitrogen atoms colored blue and carbon atoms colored yellow. This figure was prepared using the program PYMOL (www.pymol.org). (b) Stable COS-7 transfects expressing E1271K mutant *MET* were cultured in 0.5% bovine serum albumin-containing serum-free media for 16 h, then incubated with increasing concentrations of the MET inhibitors SU11274 (top) and PHA665752 (bottom) as indicated, in the presence of HGF stimulation (50 ng/ml). Whole-cell lysates were extracted for immunoblotting using antibodies against p-MET (Y1234/Y1235), MET, p-AKT, AKT, p-ERK1/2, ERK1/2 and β-actin. Wild-type *MET*-expressing COS-7 transfectant cells were included as control. E1271K mutation of MET increased the sensitivity of MET kinase phosphorylation inhibition by PHA665752.

somatic mutations identified in kinases among human cancers (Figure 7). We have conducted a complete and comprehensive survey throughout the entire human kinome for mutations identified at the conserved Glu(E)–Arg(R) ion pair in COSMIC. We also documented here the hits identifying mutations clustered in the vicinity of the ion pair, 30 amino acids proximal or distal to the Glu(E) or Arg(R). Interestingly, several kinases within the kinome were found to have mutations occurred at the Glu(E) residue, homologous to the E884–EGFR residue. These include KIT (E839K), RET (E921K), STK11/LKB1 (E223*). These are all known cancer-associated kinases that have dysregulated signaling in various human cancers, including GIST and hematological malignancies (KIT), papillary thyroid cancer (multiple endocrine neoplasm syndrome type 2) (RET) and lung cancer (RET, LKB1).

Discussion

In the era of molecularly targeted therapeutics in cancer therapy, the impact of cancer-associated mutations on kinase inhibitor sensitivity-resistance has increasingly

A[a]

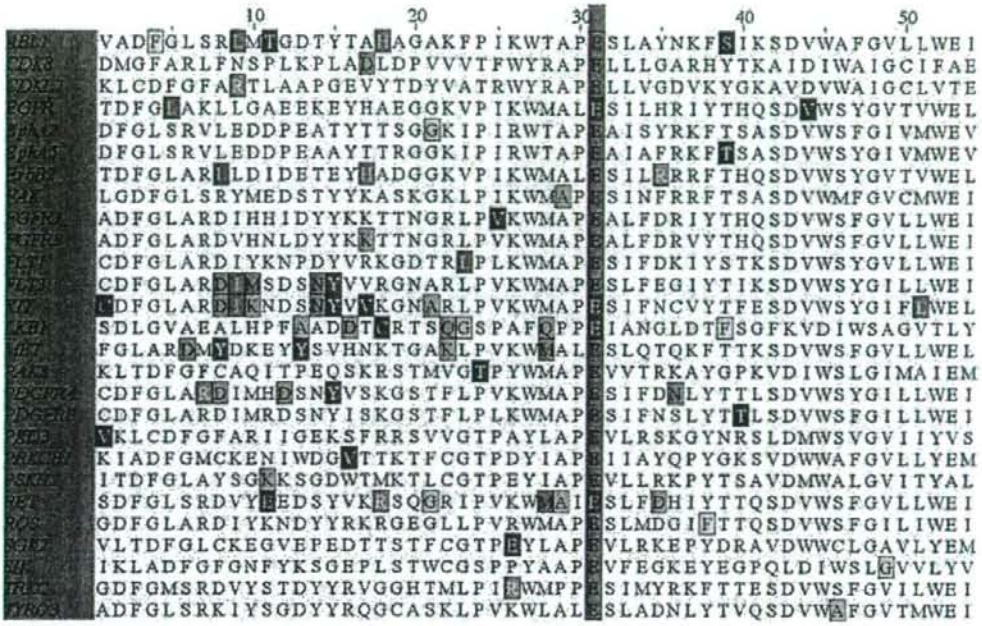

b

GENES	Mutations
ABL1:	F382L, L387M, T389A, H396P, H396R, S417Y
CDK8:	D189N
CDKL2:	R149Q
EGFR:	L858R, ***E884K***, V897I
EPHA2:	G777S
EPHA5:	T856I
ERBB2:	L869Q, H878Y, R896C
FAK:	***A612V***
FGFR1:	V664L
FGFR3:	K650E, K650M, K650Q, K650T
FLT1:	L1061V
FLT3:	D835E, D835F, D835H, D835N, D835V, D835Y, I836F, I836M, I836S, M837P, N841H, N841K, Y842C
KIT:	C809G, C809R, A814S, A814T, D816A, D816E, D816F, D816G, D816H, D816I, D816N, D816V, D816Y, I817V, K818R, D820E, D820G, D820H, D820N, D820V, D820Y, N822H, N822K, N822T, N822Y, Y823C, Y823D, Y823N, V825A, V825I, A829P, ***E839K***, L859P
LKB1:	A205T, D208N, C210*, Q214*, G215D, ***Q220****, ***E223****, F231L
MET:	D1246H, Y1248C, Y1248H, Y1253D, K1262R, ***M1268I***, ***M1268T***
PAK3:	T425S
PDGFRA:	R841S, D842*, D842I, D842V, D842Y, D846Y, Y849C, N870S
PDGFRB:	T882I
PKD3:	V716M
PRKCB1:	V496M
PSKH2:	K212I
RET:	E901K, R908K, G911D, ***M918T***, ***A919V***, ***E921K***, D925H
ROS:	F2138S
SGK2:	E259K
SIK:	G211S
TRKC:	R721F
TYRO3:	A709T

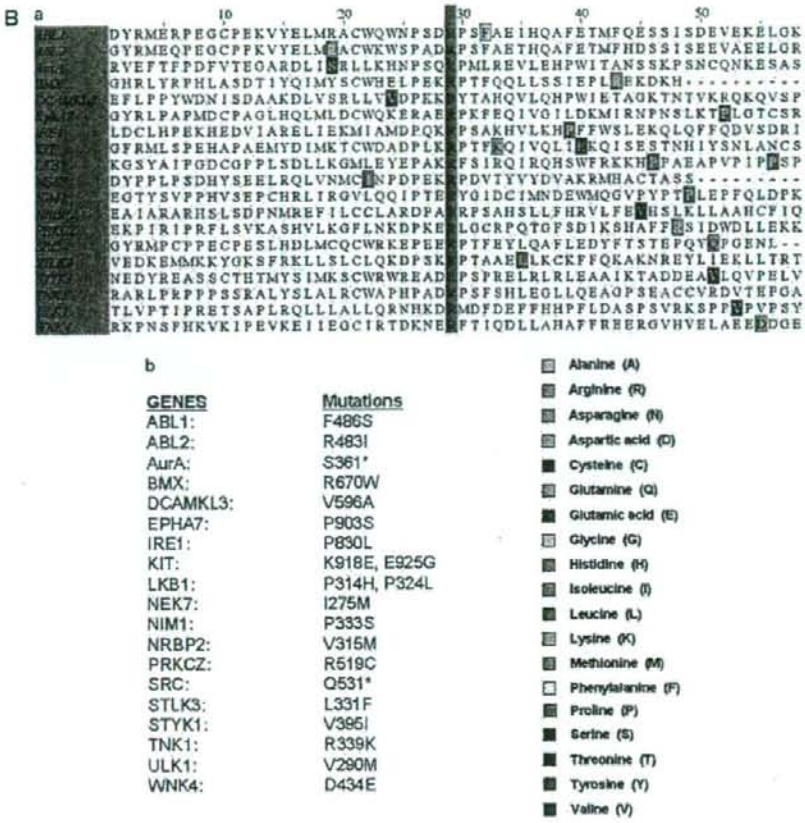

Figure 7 Continued.

important implications in the success of novel targeted inhibitors such as erlotinib (EGFR-TKI). Furthermore, knowledge of mutational correlation with inhibitor sensitivity-resistance would most likely facilitate more effective and 'personalized' targeted therapeutics development in cancer therapy. The clinical course of the patient where the somatic E884K mutation was identified (Choong *et al*., 2006) suggested that different mutations of a target kinase, such as EGFR, may lead to differential responses to targeted kinase inhibitors. Alternatively, one may postulate that there might be differences in cerebrospinal fluid penetrance by TKIs that could potentially account for central nervous system failure with disease progression in the compartment on therapy (Jackman *et al*., 2006). Our biochemical studies here now show that E884K mutation in-*cis* with L858R differentially altered inhibitor sensitivity when compared with L858R alone, through differential inhibition of the pro-survival AKT and STAT3 signaling pathways associated with altered induction of cleaved-PARP(Asp214). This is also shown to occur in an inhibitor-specific manner within the class of various

Figure 7 Survey of identified mutations at the conserved salt bridge ion pair in the human kinome (COSMIC). The COSMIC database for the human cancer genome resequencing was surveyed and screened for potential mutations identified at or near the conserved Glu(E) Arg(R) salt bridge ion pair in the human kinome. (A) (a) Glu(E)884-EGFR and analogous alignment in the kinome. (b) List of the mutations identified in the kinome is included as reference. (B) (a) Arg(R)958-EGFR and analogous alignment in the kinome. (b) List of the mutations identified in the kinome is included as reference. The color code for the amino acids is included here. We have identified several kinases within the kinome that have mutations occurred at the Glu (E) residue, homologous to the E884-EGFR. These include KIT (E839K), RET (E921K) and LKB1 (E223*). These are all known oncogenic kinases that have dysregulated signaling in various human cancers, including GIST and hematological malignancies (KIT), papillary thyroid cancer (multiple endocrine neoplasm syndrome type 2) (RET) and lung adenocarcinoma (RET, LKB1). Whereas *KIT* and *RET* are oncogenes, *LKB1* has been shown to be a tumor-suppressor gene in lung cancer, and here we showed clustering of truncation mutations at and near the salt bridge ion pair as a result of a number of mostly nonsense mutations among some missense mutations. Although no mutation at E1271-*MET* was found, there are frequent clustered hotspots of mutations at its close vicinity: three amino-acid residues proximally at M1268 (M1268T/I). This is a known activating mutation of *MET* frequently associated with metastatic lesions promoting tumor motility and progression. The selected kinases with positive 'mutational hits' in our kinome bioinformatics screen are shown here for illustration.

ERBB family small-molecule inhibitors, including reversible single EGFR or dual inhibitors (gefitinib, erlotinib, lapatinib, 4557W, GW583340 and Tyrphostin-AG1478) and irreversible EGFR inhibitor (CL-387,785).

Moreover, the E884K alone and L858R + E884K double-mutant EGFR remained sensitive to EGF, and the E884K mutation cooperates with L858R when in-*cis* to enhance the mutational effects on downstream phosphoprotein activation. To date, essentially all mutational combinations involving L858R studied were found to exist in-*cis*, suggesting potential *cis* mutation-to-mutation cooperation in EGFR signaling and possibly tumorigenesis (Tam *et al.*, 2006). Interestingly, the double mutation L858R + E884K conferred a distinctly more sensitive response to EGF stimulation selectively in the MAPK-ERK1/2 cell proliferation pathway compared with either wild type, E884K alone or L858R alone. Hence, the double mutation L858R + E884K modulated downstream EGFR signaling differentially with distinctly different effects on the AKT (downregulated) and MAPK-ERK1/2 phosphorylation (upregulated). Moreover, E884K had a dominant effect over L858R, when in-*cis*, in these signaling modulatory effects. E884K, alone or in-*cis* with L858R, can also mediate induction of p-STAT3 (pY705) (important for STAT3 dimerization and transcriptional activation of target genes) and may have a role in differential regulation of STAT3 activation and thus nuclear translocation for transcriptional activity (Lo *et al.*, 2005). Our data also share some similarities to the recent findings that various activating 'gain-of-function' mutations of FLT3 showed differential downstream signaling activation along the STAT3, STAT5, AKT and MAPK-ERK1/2 pathways, whereas all induced FLT3 kinase activation constitutively (Frohling *et al.*, 2007). *EGFR* somatic doublet mutations are potentially more frequent than understood previously, with majority of them representing driver/driver mutations rather than driver/passenger mutations (Chen *et al.*, 2008). Future kinome-targeted therapies should take into account oncogenic effects of doublet mutations in the targets, and detailed analysis of the identified doublet mutations would be warranted.

Through sequence bioinformatics and structural analysis, we identified that the E884–R958 ion pair in EGFR kinase domain is highly conserved, by both sequence homology and structural salt-bridge formation, across the entire human kinome. Many of the protein kinases in the human kinome are 'druggable' therapeutic targets for various human cancers (Krause and Van Etten, 2005; Ma *et al.*, 2005a). This striking finding provides a structural basis for the potential mechanism of alteration of substrate specificity. This hypothesis is substantiated by our study using mutational disruption of the E884–R958 ion pair through an R958D substitution resulting in an opposite electrostatic charge between the wild-type and the mutant residue at codon 958. Similar differential sensitivity toward gefitinib (more sensitive) and erlotinib (more resistant) was observed in our *in vitro* EGFR inhibition study here. It is interesting to note that this salt bridge is located directly between two regions critical for normal EGFR activation, the intermolecular EGFR activation interface and the activation loop. Residue R958 falls between helices αH and αI and is proximal to the intermolecular EGFR activation interface recently revealed by structure-directed studies (Zhang *et al.*, 2006). Residue E884 is the conserved glutamate of the MALE motif (MAPE in PKA) and falls within helix αEF at the C terminus of the activation loop. This salt bridge helps to orientate helix αEF. In the recent EGFR kinase domain crystal structure bound to a peptide substrate analog (PDB accession code: 2GS6) (Zhang *et al.*, 2006), helix αEF packs against the substrate analog, suggesting that disruption of the salt bridge by an acquired E884K mutation could influence substrate recognition and binding. The acquisition of a lysine at codon 884 may therefore bring about local conformation disruptions that alter EGFR interactions with downstream substrates. Although we did not identify further E884K mutation (or any mutations involving R958 residue) in *EGFR* from the Japanese patients tumor sample cohort, the results of our study may have implication on the potential impact of cancer-associated mutations that may interrupt the integrity of the salt bridge of a kinase. As the human kinome is a rich source of 'druggable' targets, we extended our search through bioinformatics data-mining from the COSMIC human cancer genome resequencing project. To this end, we identified several proximal ion pair residue substitutions recorded in the COSMIC database at the E884 (EGFR) homologous residue, in the oncogenic kinases KIT and RET as well as in the tumor-suppressor LKB1 (also known as STK11). Mutations at the neighboring residues of the conserved motif MAPE(884), as exemplified in FAK-A612V, MET-M1268I/T, RET-M918T and RET-A919V, as well as the truncational nonsense mutation in LKB1-Q220*, were also identified from the COSMIC database. Furthermore, the juxtaposing proximal region to the MAPE(884) conserved motif in the kinome also appears to harbor mutational hotspots in the human cancer genome. Nonetheless, the significance of these mutations with respect to the kinase structure and signaling function is not clear. Although KIT has been extensively characterized with an established oncogenic role in some hematological malignancies and GIST, it has not been found to play a key role in lung cancer. However, recent studies have implicated interesting oncogenic role of RET (Thomas *et al.*, 2007), FAK (Ma *et al.*, 2007; Rikova *et al.*, 2007), MET (Ma *et al.*, 2005a) and tumor-suppressor role of LKB1 (Ji *et al.*, 2007) in lung cancer.

Recently, better understanding of signaling network interactions between EGFR and MET is beginning to emerge (Guo *et al.*, 2008; Tang *et al.*, 2008). MET genomic oncogenic amplification has also been identified to correlate with acquired resistance to EGFR inhibitors (gefitinib/erlotinib) with or without T790M-*EGFR* mutation (Bean *et al.*, 2007; Engelman *et al.*, 2007). Numerous kinase domain mutations of *MET* have been identified in previous studies, many of them shown to be activating and most frequently found in

metastatic tumor lesions compared with the primaries (Di Renzo *et al.*, 2000). The E1271–MET conserved ion pair residue occurs within the conserved MALE motif, where M1268 is a mutational hotspot frequently found substituted in human cancers (M1268T/I). This is a known activating mutation of *MET* frequently associated with metastatic lesions promoting tumor motility and progression. Our results here demonstrate that E1271K-MET effectuated differential effect on sensitivity toward the two preclinical MET inhibitors, SU11274 (unchanged) and PHA665752 (sensitizing). Hence, mutations in the kinase domain of MET may play a role in modulating the inhibitory spectrum of MET inhibitors, similar to what is established in EGFR-targeted therapy using gefitinib/erlotinib. Whether these mutationally specific differences in inhibitor sensitivity would eventually be clinically relevant is not clear at present and should be a focus of future research. MET is emerging as an important therapeutic target in cancer therapy beyond EGFR. More detailed studies to better define the relative role of kinase mutations in *MET* and how they can modulate inhibitor sensitivity would be warranted. Furthermore, nonkinase mutations of *MET*, in the extracellular sema domain and the short cytoplasmic juxtamembrane domain, have been identified to be important in lung cancer and mesothelioma (Ma *et al.*, 2003a, 2005a; Jagadeeswaran *et al.*, 2006). Little is known about the correlation of inhibitor sensitivity with these nonkinase mutations, and they should be included in future studies. Bellon *et al.* (2008) recently compared the crystal structures of a novel MET inhibitor AM7, and that of SU11274 when bound to the unphosphorylated form of MET kinase. They identified a novel binding mode of a MET inhibitor AM7 compared with SU11274 and raised the possibility of designing TKIs that have improved specific activity and specificity toward different mutant profiles in different cancers; hence 'mutationally-targeted inhibitors'.

Although the role of kinase domain mutations in modulating the sensitivity-resistance to small-molecule inhibitors, in the case of BCR/ABL, KIT and EGFR, has been quite extensively studied, in-depth understanding of the relative role of mutations in other target kinases, such as MET, RET and FAK in determining specific inhibitor sensitivity is still largely lacking. The ion pair formed by residues E884 and R958 in the EGFR kinase domain is a highly conserved feature in the human kinome, and mutations of this conserved ion pair may result in conformational changes that alter kinase substrate recognition. The discovery that disruption of the conserved E884–R958 ion pair affects EGFR signal transduction and inhibitor sensitivity indicates the clinical importance of *in vitro* and biochemical analysis for all documented resistance mutations. Our analysis also suggests that targeted therapy using small-molecule inhibitors should take into account potential cooperative effects of multiple intramolecular kinase mutations. As the number of targeted TKIs available increases, it is anticipated that a 'personalized' approach to cancer therapy on the basis of knowledge of the activating mutations present should improve the efficacy of these treatments.

Materials and methods

Plasmid constructs and site-directed mutagenesis
The plasmids pcDNA3.1 containing the full-length wild-type *EGFR* and the L858R-*EGFR* cDNA insert was a generous gift from Dr Stanley Lipkowitz (NIH/NCI). The generation of the kinase domain missense mutations of *EGFR*, E884K, L858R + E884K and L858R + R958D were performed using the QuikChange Site-Directed Mutagenesis XL II kit (Stratagene, La Jolla, CA, USA) as described previously (Choong *et al.*, 2006). The E1271K mutation of *MET* was introduced into the wild-type *MET* plasmid (Ma *et al.*, 2003a). Incorporation of the correct mutations was confirmed by direct DNA sequencing of the constructs.

Cell culture and transfection
COS-7 cells were grown as described previously (Choong *et al.*, 2006). Transfection method was described in Supplementary Materials and methods.

Cell proliferation and cytotoxicity assays
Cell proliferation and cytotoxicity assays were performed using tetrazolium compound-based CellTiter 96 AQ_{ueous} One Solution Cell Proliferation (MTS) assay (Promega) (see Supplementary Materials and methods).

Preparation of cell lysates and immunoblotting
Whole-cell lysates were extracted, separated by 7.5% SDS–polyacrylamide gel electrophoresis , immunoblotted using the various primary antibodies indicated and developed with SuperSignal West Pico Chemiluminescent Substrate (Pierce, Rockford, IL, USA) as described previously (Choong *et al.*, 2006). The following primary antibodies were used: phosphotyrosine (4G10, Upstate Biotechnology, Lake Placid, NY, USA), phospho-EGFR (Y1068) (BioSource International, Camarillo, CA, USA), EGFR (Santa Cruz Biotechnology, Santa Cruz, CA, USA), phospho-STAT3 (Y705) (Cell Signaling, Danvers, MA, USA), STAT3 (Zymed, South San Francisco, CA, USA), phospho-AKT (S473) (Cell Signaling), AKT (Biosource International), phospho-ERK1/2 (T202/Y204) (Cell Signaling), ERK1/2 (Biosource International), cleaved-PARP(Asp214) (cleaved-poly (ADP-ribose) polymerase (Asp214)) (Cell Signaling) and β-actin (Santa Cruz Biotechnology).

Chemicals
The details regarding the EGFR TKIs and MET TKIs used in this study are described in the Supplementary Materials and methods.

Lung tumor genomic DNA extraction and DNA sequencing
Genomics DNA was extracted using standard techniques from 67 non-small-cell lung cancer patients treated from July 1995 to March 2003 at Osaka Prefectural Medical Center for Respiratory and Allergic Disease (Osaka, Japan). All tumor samples were used in accordance with Institutional Review Board protocol, with patients' informed consent wherever necessary. Screening for mutations within exon 22 (harboring E884) and exon 23 (harboring R958) was performed using standard single-strand conformational polymorphism analysis, followed by direct DNA sequencing when indicated (for details, see Supplementary Materials and methods).